

University of Southern Queensland
Faculty of Health, Engineering and Sciences

Remote Identification of Overhead Conductor Materials

A dissertation submitted by

Scott A Marsh

In fulfilment of the requirements of

ENG4111/ENG4112 Research Project

Towards the degree of

Bachelor of Engineering (Power)

Submitted: October 2015

Abstract

The recent draft determination by Australian Energy Regulator has meant a probable large reduction of approximately 30% in the income able to be generated by Ergon Energy. This recent ruling has increased the focus on cost effective and timely solutions to problems and encouraged continual evaluation of emerging technology which may facilitate these solutions. This focus has become a primary consideration in the organisation.

The five main types of conductor present in the Ergon Energy bare overhead network in copper, galvanised steel, steel re-enforced aluminium, aluminium and aluminium alloy, which all age in a variety of ways when exposed to the elements. With over 1,800 circuit kilometres of unidentified conductor in the Ergon Energy network and a further unknown amount of incorrectly identified conductor, suitably managing the risk of conductor failure in a targeted, efficient, and timely manner is problematic.

Spectral analysis is rapidly maturing as a technology with recent uses including satellite imagery to identify mineral deposits, analysis of distant planets, and also includes uses such as identifying cancerous growths in the human body, identifying scrap metals, evaluating the contamination of land by various contaminants, and helping naval vessels avoid mines by identification of these metal objects in the ocean.

Initial measurements in the visible spectrum were taken with a low cost commercial USB plug and play spectrometer which identified significant differences in the spectral responses of copper, steel and aluminium. This spectrometer gave relatively constant results for aluminium, and galvanised steel under various lighting conditions, sample ages, and sample sizes. Consistent results were also obtained of various copper sample sizes and lighting conditions, however the variable surface patina's due to weathering resulted in inconsistent results. The spectrometer could not discern between all aluminium conductor (AAC) and all aluminium alloy conductor (AAAC).

An attempt was made to build an image spectrometer from a Nikon D700 consumer camera which was partially successful. The device was successful in recording relatively accurately the dominant wavelengths of a compact fluorescent light source and did record two measurements of aluminium conductor with moderate accuracy. Difficulties were encountered with aligning the optical path, and artefacts being introduced in the optical path.

Limitations of Use

University of Southern Queensland
Faculty of Health, Engineering and Sciences
ENG4111/ENG4112 Research Project

Limitations of Use

The Council of the University of Southern Queensland, its Faculty of Health, Engineering & Sciences, and the staff of the University of Southern Queensland, do not accept any responsibility for the truth, accuracy or completeness of material contained within or associated with this dissertation.

Persons using all or any part of this material do so at their own risk, and not at the risk of the Council of the University of Southern Queensland, its Faculty of Health, Engineering & Sciences or the staff of the University of Southern Queensland.

This dissertation reports an educational exercise and has no purpose or validity beyond this exercise. The sole purpose of the course pair entitled “Research Project” is to contribute to the overall education within the student’s chosen degree program. This document, the associated hardware, software, drawings, and other material set out in the associated appendices should not be used for any other purpose: if they are so used, it is entirely at the risk of the user.

Professor Lyn Karstadt

Executive Dean

Faculty of Health, Engineering and Sciences

Certification

I certify that the ideas, designs and experimental work, results, analyses and conclusions set out in this dissertation are entirely my own effort, except where otherwise indicated and acknowledged.

I further certify that the work is original and has not been previously submitted for assessment in any other course or institution, except where specifically stated.

Scott A Marsh

001220726

Signature

Date

Acknowledgements

I would like to acknowledge and thank:

Dr Leslie Bowtell – Faculty of Health, Engineering and Science, USQ.

Mr Dave Shephard – Regional Asset Manager Ergon Energy.

Mr Paul Hohenhaus – Protection Standards Ergon Energy and long-time study buddy.

Katrina, Connor, Ashleigh Marsh – Long suffering family.

Table of Contents

ABSTRACT	I
LIMITATIONS OF USE	II
CERTIFICATION	III
ACKNOWLEDGEMENTS	IV
TABLE OF CONTENTS	V
LIST OF TABLES	IX
LIST OF FIGURES	X
NOMENCLATURE	XII
GLOSSARY	XIII
1. INTRODUCTION	1
1.1. Chapter Overview	1
1.2. Background	1
1.2.1. Spectroscopy	2
1.2.2. Traditional Spectroscopy v Image Spectroscopy	5
1.3. Project Justification	8
1.3.1. Current conductor identification methods	9
1.3.2. Cost of current identification methods	10
1.3.3. Overhead Conductors	11
1.3.3.1. Common conductor types	11
1.3.3.2. Conductor risk profiles	12
1.4. Project Objectives	18
1.5. Chapter Overview	19

1.6.	Limitations & Restrictions	20
1.7.	Chapter Summary	20
2.	LITERATURE REVIEW	21
2.1.	Chapter Overview	21
2.2.	Reflectance transmittance emittance and absorption.	21
2.3.	Factors affecting spectral reflectance measurements.	23
2.4.	Quality criteria for reflectance measurements.	26
2.5.	Analysis of an inexpensive means of spectral photography as proof of concept	27
2.5.1.	CTIS and Fourier Transformation of the Image Data.	30
2.6.	Relevant Australian Standards	34
2.6.1.	Australian Standard AS3607 – 1989 Conductors-Bare overhead, aluminium and aluminium alloy-steel reinforced.	34
2.6.2.	Australian Standard AS 2848.1 – 1998 Aluminium and aluminium alloys – Compositions and designations – Wrought products.	35
2.6.3.	Australian Standard AS 1746-1991 Conductors – Bare overhead – Hard-drawn copper.	37
2.6.4.	Australian Standard AS 1279-1985 Copper refinery shapes.	37
2.6.5.	Australian Standard AS1574-1984 Copper and copper alloys – Wire for electrical purposes.	38
2.7.	Chapter Summary	39
3.	METHODOLOGY	40
3.1.	Chapter Overview	40
3.2.	Research	40
3.3.	Measurements using a commercial spectrometer	40
3.4.	Confirmation of theory using image spectroscopy	44
4.	RESULTS AND DISCUSSION	49
4.1.	Chapter Overview	49
4.2.	Commercial USB plug and play spectrometer results	49

4.2.1.	Galvanised Steel under spotlight	49
4.2.1.	Galvanised steel conductors under fluorescent and low level daylight	50
4.2.1.	Copper conductors under spotlight	51
4.2.1.	Copper conductors under fluorescent and low level daylight	52
4.2.1.	All aluminium conductors under spotlight	53
4.2.2.	All aluminium conductors under fluorescent and low level daylight	54
4.2.3.	Comparison of all aluminium conductors and all aluminium alloy conductors under spotlight	54
4.3.	Consumer camera image spectroscopy results	54
4.3.1.	Establishing the calibration of the results of the Image spectroscopy implementation	54
4.3.1.	Measurements using the Image spectroscopy implementation	56
5.	CONCLUSIONS & RECOMMENDATIONS	59
5.1.	Chapter Overview	59
5.2.	Achievement of the Project Objectives	59
5.3.	Feasibility	62
5.4.	Recommendations / Further Work	62
	REFERENCES	64
	BIBLIOGRAPHY	64
	APPENDIX A: PROJECT SPECIFICATION	68
	APPENDIX B: OCEAN OPTICS USB4000 SPEC SHEET	69
	APPENDIX C: NIKON D700 SPEC SHEET	70
	APPENDIX D: OCEAN OPTICS USB4000 – GALVANISED STEEL CONDUCTOR UNDER HALOGEN SPOTLIGHT	71
	APPENDIX E: OCEAN OPTICS USB4000 – GALVANISED STEEL CONDUCTOR UNDER HALOGEN SPOTLIGHT, FLUORESCENT, AND LOW LEVEL DAYLIGHT	72

APPENDIX F: SPECTROSCOPY USING AN OCEAN OPTICS USB4000 – COPPER CONDUCTOR UNDER HALOGEN SPOTLIGHT	73
APPENDIX G: SPECTROSCOPY USING AN OCEAN OPTICS USB4000 – ALUMINIUM CONDUCTOR UNDER HALOGEN SPOTLIGHT	74
APPENDIX H: OCEAN OPTICS USB4000 – ALL ALUMINIUM CONDUCTOR UNDER HALOGEN SPOTLIGHT, FLUORESCENT, AND LOW LEVEL DAYLIGHT	75
APPENDIX I: OCEAN OPTICS USB4000 – ALL ALUMINIUM CONDUCTOR AND ALL ALUMINIUM ALLOY CONDUCTOR UNDER HALOGEN SPOTLIGHT	76
APPENDIX J: IMAGE SPECTROSCOPY USING A CONSUMER CAMERA – CONFIRMATION OF CONCEPT	77
APPENDIX K: SPECTROSCOPY USING AN OCEAN OPTICS USB4000 – ALL CONDUCTORS	78

List of Tables

TABLE 1. MASS OF ZINC COATING FOR STEEL WIRES (AUSTRALIAN STANDARDS 1989)	34
TABLE 2. MINIMUM MASS OF ALUMINIUM COATING FOR STEEL WIRES (AUSTRALIAN STANDARDS 1989).....	35
TABLE 3. ALLOYING ELEMENT LIMITS (AUSTRALIAN STANDARDS 1998).....	36
TABLE 4. RELATED DESIGNATIONS FOR COPPER REFINERY SHAPES (AUSTRALIAN STANDARDS 1985)	37
TABLE 5. MATERIALS, TEMPERS AND FINISHES FOR COPPER AND COPPER ALLOYS (AUSTRALIAN STANDARDS 1984)	38
TABLE 6. ELECTRICAL RESISTIVITY OF PLAIN WIRE (AUSTRALIAN STANDARDS 1984).....	39
TABLE 7. CORRELATION CO-EFFICIENTS FOR GALVANISED STEEL REFLECTANCE CURVES UNDER SPOTLIGHT.....	50
TABLE 8. CORRELATION CO-EFFICIENTS FOR GALVANISED STEEL REFLECTANCE CURVES UNDER FLUORESCENT AND LOW LEVEL DAYLIGHT.....	51
TABLE 9. CORRELATION CO-EFFICIENTS FOR COPPER REFLECTANCE CURVES UNDER SPOTLIGHT	51
TABLE 10. CORRELATION CO-EFFICIENTS FOR COPPER REFLECTANCE CURVES UNDER FLUORESCENT AND LOW LEVEL DAYLIGHT	52
TABLE 11. CORRELATION CO-EFFICIENTS FOR ALL ALUMINIUM REFLECTANCE CURVES UNDER SPOTLIGHT	53
TABLE 12. CORRELATION CO-EFFICIENTS FOR ALL ALUMINIUM REFLECTANCE CURVES UNDER FLUORESCENT AND LOW LEVEL DAYLIGHT	54
TABLE 13. CORRELATION CO-EFFICIENTS FOR ALL ALUMINIUM AND ALUMINIUM ALLOY REFLECTANCE CURVES USING BOTH MEASURING INSTRUMENTS (OO DENOTES THOSE MEASURED WITH THE USB4000).....	58

List of Figures

FIGURE 1: THE ELECTROMAGNETIC SPECTRUM (LEVERINGTON 2001). THE VISIBLE AND NEAR-INFRARED WAVELENGTHS ARE DOMINATED BY REFLECTED SOLAR RADIATION.....	3
FIGURE 2: A FULL WIDTH AT HALF MAXIMUM (FWHM) OF 10 NM GAUSSIAN PROFILE TYPICAL OF MODERN SPECTROMETERS (CURTISS & GOETZ 2001).	4
FIGURE 3: TYPICAL LAYOUT OF A MODERN USB POWERED SPECTROMETER (HTTP://WWW.SPECTRALPRODUCTS.COM/SPECTROMETER).	6
FIGURE 4: TYPICAL OPERATION OF AN IMAGE SPECTROMETER (COURTESY NEMO PROJECT OFFICE, UNITED STATES NAVY) ..	7
FIGURE 5: VARIOUS SPECTRAL MEASUREMENTS BY ACCURACY (HTTP://WWW.MARKELOWITZ.COM/HYPERSPECTRAL.HTML) .	8
FIGURE 6: TOP FIVE P2 CONDUCTOR DEFECTS TRENDED OVER TIME	14
FIGURE 7: CONDUCTOR P1 DEFECTS 08/09 – 12/13.....	15
FIGURE 8: CONDUCTOR P2 DEFECTS 08/09 – 12/13	15
FIGURE 9: TOP FIVE P2 CONDUCTOR DEFECTS TRENDED OVER TIME	16
FIGURE 10: CREATING PARALLEL PROJECTIONS BY DIFFRACTING THE IMAGE (CTIS)	29
FIGURE 11: REPRESENTATION OF THE CTIS IMAGE CUBE AND DECK OF CARDS ANALOGY (HAGEN, DERENIAK & SASS 2007).	32
FIGURE 12: REPRESENTATION OF A SINGLE PIXEL BEING BACKPROJECTED INTO THE DATACUBE IN SINGLE PROJECTION IN (A) AND A SET OF FOUR PROJECTIONS IN (B) (HAGEN, DERENIAK & SASS 2007).	33
FIGURE 13: SPECTROMETER FIELD OF VIEW CALCULATIONS (HTTP://DISCOVER.ASDI.COM/BID/97740/EXPERT-TIP-UNDERSTAND-YOUR-FIELD-OF-VIEW-WHEN-TAKING-REFERENCE-MEASUREMENTS)	41
FIGURE 14: ACTUAL SETUP FOR SPECTRAL MEASUREMENTS USING AN OCEAN OPTICS USB 4000.	42
FIGURE 15: THE RANGE OF CONDUCTORS TESTED	43
FIGURE 16: THE ORIGINAL NIKKOR 35-105MM LENS ON LEFT AND 100MM ACHROMATIC LENS ON RIGHT	45
FIGURE 17: THE ASSEMBLED CONSUMER CAMERA	46
FIGURE 18: A REPRESENTATION OF THE OPTICAL PATH REQUIRED TO SUCCESSFUL MEASUREMENTS.	46

FIGURE 19: A CLOSE UP PHOTOGRAPH SHOWING THE TYPICAL SURFACE CHARACTERISTICS OF THE ACTUAL GALVANISED STEEL CONDUCTORS TESTED.	50
FIGURE 20: A CLOSE UP PHOTOGRAPH SHOWING THE DIFFERENT SURFACE CHARACTERISTICS OF THE ACTUAL COPPER CONDUCTORS TESTED.	52
FIGURE 21: A CLOSE UP PHOTOGRAPH SHOWING THE TYPICAL SURFACE CHARACTERISTICS OF THE ACTUAL ALUMINIUM AND ALUMINIUM ALLOY CONDUCTORS TESTED.	53
FIGURE 22: FLUORESCENT SPECTRUM SOURCE: ASTER SPECTRAL LIBRARY BALDRIDGE, A. M., S.J. HOOK, C.I. GROVE AND G. PP. 711-715.....	55
FIGURE 23: FLUORESCENT SPECTRUM MEASUREMENT USING AN IMAGE SPECTROMETER CREATED FROM A CONSUMER CAMERA.	56
FIGURE 24: SPECTRAL MEASUREMENT USING AN IMAGE SPECTROMETER CREATED FROM A CONSUMER CAMERA.THE DATA CUBE WAS CONSTRUCTED FROM THIS MEASUREMENT.	57
FIGURE 25: MEASUREMENT OF SOME 140 MM X 20 MM BOLTS AT 300 METRES USING THE LEICA NOVA MS50 (COURTESY OF C. R. KENNEDY SURVEY).....	61

Nomenclature

Term	Description	Units
AC	Alternating Current	A
DC	Direct Current	A
kV	kilo Volts	kV
kVA	kilo Volt Amperes	kVA
kW	Kilo Watts	kW
m	Metres	m
mm	Millimetres	mm
μm	Micrometres	μm
nm	Nanometres	nm
mm^2	Millimetres squared	mm^2

Glossary

AEMO	Australian Energy Market Operator.
CCD	“Charge coupled device” converts light photons into an electron charge, in this case used as the light/digital interface in a digital camera.
Ergon Energy	Regional Queensland’s electricity distribution network owner. A government owned corporation which supplies approximately 700,000 customers and 97% of the state’s area.
NEMO	“Naval Earth Map Observer program” US space based remote sensing system for collecting broad area hyperspectral imagery for naval forces and the civil sector.
DEE	“Dangerous electrical event” which is the coming into existence circumstances which fit specific criteria and pose a threat of injury or death.
AAC	All aluminium conductors
AAAC	All aluminium alloy conductors
SC/GZ	Steel conductor which has been galvanised
ACSR/GZ	Aluminium conductors with steel (galvanised) reinforcement
ACSR/AC	Aluminium conductors with steel (aluminium clad) reinforcement
ACSR/AZ	Aluminium conductors with steel (aluminized) reinforcement
AACSR/GZ	Aluminium alloy conductors with steel (galvanised) reinforcement
AACSR/AC	Aluminium alloy conductors with steel (aluminium clad) reinforcement
HDBC	Hard drawn bare copper
HDCC	Hard drawn cad copper
SC/AC	Steel conductor (aluminium clad)
ACSR	Smooth body compacted conductor
P1	Serious deterioration or damage, which requires some specific action or indicates an unacceptable risk of failure in the short term or presents an imminent danger or risk of asset failure. Urgent attention is required. Any defect that presents an immediate risk shall be addressed immediately. All other defects are to be:

	<ul style="list-style-type: none"> • As required, attend and make safe within 3 days of the date of inspection, and • Addressed within 30 days of the date of inspection
P2	<p>Moderate deterioration or damage, which requires some specific action or indicates an unacceptable risk to safety, environment, operations, or reliability in the medium term. Rectify defects within target timeframes;</p> <ul style="list-style-type: none"> • Ergon Energy – 9 months (39 weeks) except for suspect and unserviceable poles. <p>If this timeframe cannot be met due to access issues then suitable management of the risk of failure needs to be undertaken.</p>
GIS	Geographic information system, in Ergon Energy typically refers to the GE Smallworld package or Google Earth.
RAM	“Regional asset management” refers the group within Ergon Energy tasked with managing the network including failed in service assets, augmentation, and replacement.
CBRM	Condition based risk management
CTIS	“Computed tomography imaging spectroscopy” is a snapshot (non-scanning) method of spectral measurement.
IACS	“International annealed copper standard” is a unit of conductivity for metals and alloys relative to a standard annealed copper conductor.
HDR	“High dynamic range imaging” refers to a photographic technique which produces a high dynamic range of luminosity using multiple exposures of the same scene.
FPA	Focal plane array
PSF	Point spread function

1. Introduction

1.1. Chapter Overview

This introductory chapter presents the required background information on spectroscopy and the fundamentals of how spectroscopy works, and states the project objectives.

This chapter also justifies the need for this project including actual statistics of Ergon Energy network performance and the differing levels of risk of the conductor types. The current methods of conductor identification are investigated and an actual past business case is reviewed to better understand the costs associated with the current methods of conductor identification. The works contained in this chapter will fulfil requirement two of the specification:

2. Critically evaluate current conductor identification techniques.

1.2. Background

Image Spectroscopy technology has the potential to better facilitate the tasks mentioned above, by analysing a large spectrum (both visible and non-visible) of the reflected light to ascertain the material make-up of the object studied (in this case an overhead conductor from the ground by an unskilled resource).

Historically Ergon Energy comprised six independent regions that purchased materials and produced design requirements independently of each other. The conductor type and material specified also varied. This variation in conductor still exists on the network today and will be the largest challenge of this project.

The development of a method for unskilled resources to remotely identify conductor material has large financial benefits for an organisation such as Ergon Energy.

- At present if a conductor is classed as unknown the protection group makes an assumption the conductor is steel. This is a very conservative approach as steel is a very high impedance conductor which often results in identified reach issues and additional downstream protection devices requested. This approach is very costly as each downstream recloser to extend reach is costly approximately \$100,000 and a more accurate assessment of conductor materials will likely prevent installation of

some of these devices, or at least tens of thousands of dollars in scoping effort before the correct conductor is identified.

- Ergon Energy has made a commitment to remove all copper conductors from the network to the Queensland Government. Without a method to identify conductor material that can be used by external resources this commitment will prove very costly to the business with an initial project estimated in the tens of millions of dollars.

This project will have an outcome of proving or disproving spectral analysis as a method that can be used by an aircraft mounted device to identify conductor material without encroaching on clearances requirements to the conductors or requiring access with the associated loss of supply to customers and cost in switching and generation.

Finding a viable option for remote conductor material identification will provide Ergon Energy with a method to identify higher risk conductors such as copper and steel that can be used by relatively unskilled resources with minimum training on a state-wide basis. If spectral measurement proves to be a suitable technology, using a specifically calibrated and designed spectrometer to identify conductor materials will enable Ergon Energy to meet its commitment to the state government, allow it to identify and prioritise replacement of copper conductors, and identify high impedance conductors such as steel when protection studies are carried out on feeders across the network.

Based on these outcomes and the large amount of capital expenditure that could be saved by using such a method the project is found to be a worthy task.

1.2.1. Spectroscopy

Spectral imaging or spectroscopy is a very well researched and understood topic. The spectral output of satellite or aircraft mounted systems has been used extensively in the mapping of geological and mineralogical features for some time (Clark 1999) and has distinct advantages over conventional lower resolution imaging in that materials can actually be identified when compared against known spectral reflectance curves rather than just separated as different. Spectral imaging has however traditionally been confined to mining and other geological uses due to the cost of these systems and has been mounted in aircraft or satellites. Field based applications of this form of imaging have been explored however the technology has never been used to identify overhead conductor materials.

As photons of light enter a material they encounter the elements that make up the structure of that material. These elements scatter or refract the photons as they bounce off or enter a particle depending on the surface of the particle struck and the chemical bonds between these

particles. As these photons of light strike particle after particle some light photons are reflected away from the material and can be measured. All materials at some temperature above absolute zero also emit photons which are also reflected and refracted by particles and chemical bonds in the material. Photons of light not reflected or refracted back out of the material are said to be absorbed by that material. The wavelength of photons commonly absorbed by a material is dependent on several characteristics of the material so it follows that information about the type of material being observed can be derived by which wavelengths of light that are reflected and absorbed by it.

The human eye is form of spectrometer which can detect only a very narrow band of the available wavelengths. Items such as timber look commonly a brown colour due to the wavelengths of light which the timber reflects and refracts back to the eye.

The four terms used to describe the spectrometer capability are:

- Spectral Range which breaks the spectrum up into 5 recognised bands which are:
 - Ultraviolet (UV) 0.001 – 0.4 μm
 - Visible 0.4 – 0.7 μm
 - Near Infra-red (NIR) 0.7 – 3 μm
 - Mid infra-red (MIR) 3 – 30 μm
 - Far infra-red (FIR) 30 μm – 1 mm

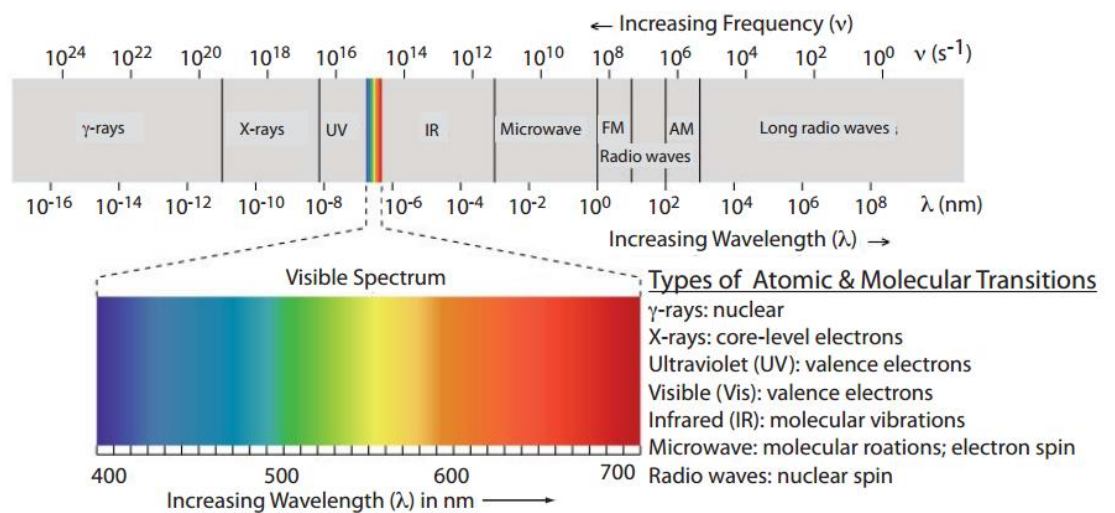


Figure 1: The electromagnetic spectrum (Leverington 2001). The visible and near-infrared wavelengths are dominated by reflected solar radiation.

- Spectral Bandwidth which is the amount of the spectrum the spectrometer can accurately measure in each channel. A spectrometer has a number of channels so if

the bandwidth is small and the channels are arranged next to each other the spectrometer has a finer granularity to the resulting spectral curve measured by each channel. Ideally each bandwidth will have a bandpass profile which accepts no light from outside its bandwidth. Unfortunately due to inadequate blocking filters and stray photons within the device, light is introduced from outside the narrow band intended giving the bandpass profile a distinct Gaussian profile. The definition of the bandpass is the width of the wavelength captured at the 50% response level of the function, otherwise known as the Full Width at Half Maximum (FWHM).

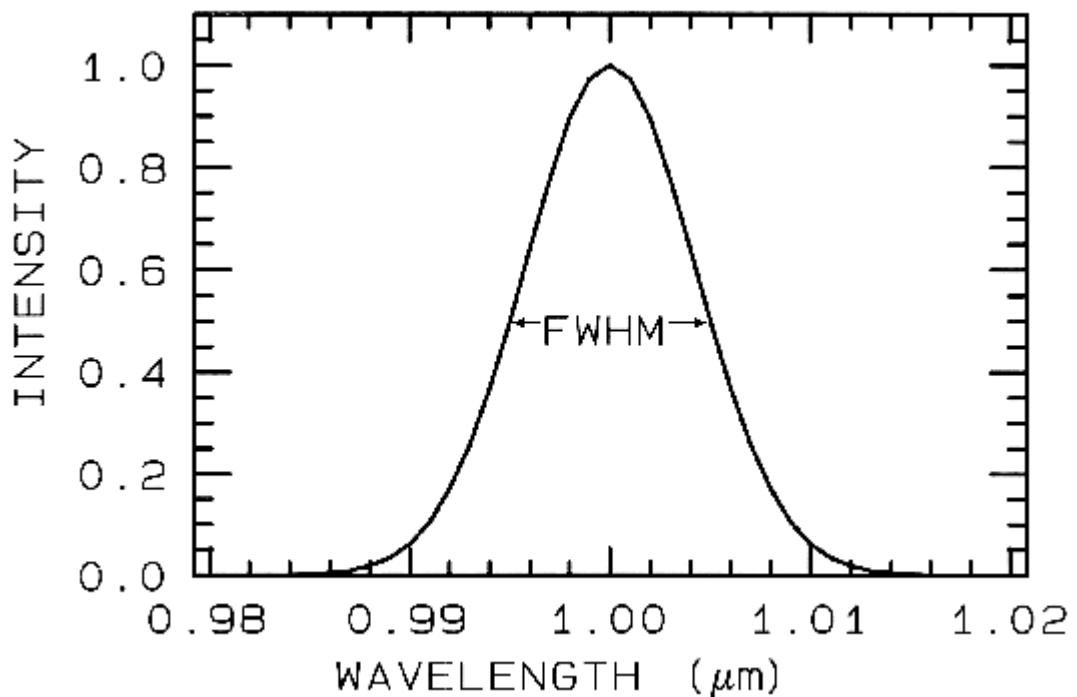


Figure 2: A full width at half maximum (FWHM) of 10 nm Gaussian profile typical of modern spectrometers (Curtiss & Goetz 2001).

- Spectral sampling is the distance between the spectral bandwidth channels in wavelength and together with the spectral bandwidth describes the resolution of the device. The theory of information states that two samples are required if we have two unknown spectral features. According to the Nyquist theorem sampling at 50% of FWHM results in the maximum information obtained.
- Signal to noise ratio is an indication of how precise the spectrometer can measure the spectral curve and depends on how pronounced the identifying spectral features are, how strong the light reflected from the subject is, the detector sensitivity, and the spectral bandwidth.

Reflectance and emittance spectroscopy measure the photons reflected in any material irrespective of whether the material is a gas, liquid or a solid and relies on the effect the chemical bonds in the material has on the path of incoming photons and emitted photons and can be applied to either crystalline or amorphous materials. As long as the photons are received by the measuring device the distance from the subject being measured is irrelevant. The Spectrometer can be on the same bench as the subject in the lab, or across the other side of the solar system from a planet to be measured.

Historically the very high sensitivity of spectroscopy was the main disadvantage of the technique, with the very wide range of chemical bonds due to the almost unlimited manner in which particles make up the objects around us. This variety of material makeup results in sometimes extremely complex spectral curves. This complexity is due to the chemical composition of some materials and historically resulted in the obtained spectral measurement considered unintelligible yielding no usable information. Research into the area and the advances in computing power allowing the processing of large amounts of information in a timely manner have turned this disadvantage into an advantage. Those spectral signatures that were thought to be too complex to yield any useful information are now being understood and give very detailed and accurate insights into a materials makeup.

1.2.2. Traditional Spectroscopy v Image Spectroscopy

Traditional spectroscopy as in the measurements taken with the Ocean Optics USB4000 spectrometer in this project, uses a primary lens to funnel all available light photons and focus them at the slit or square aperture. This slit or square is what is ultimately imaged onto the sensor of the device and does not allow stray light photons from other sources that fall outside this opening to progress any further in the optical path. Further lenses then collimate (or make parallel) the light photons and directs them onto the diffraction grating. The diffraction grating disperses the parallel light photons into their various wavelengths and arranges them at slightly different angles so they fall onto the detector separately.

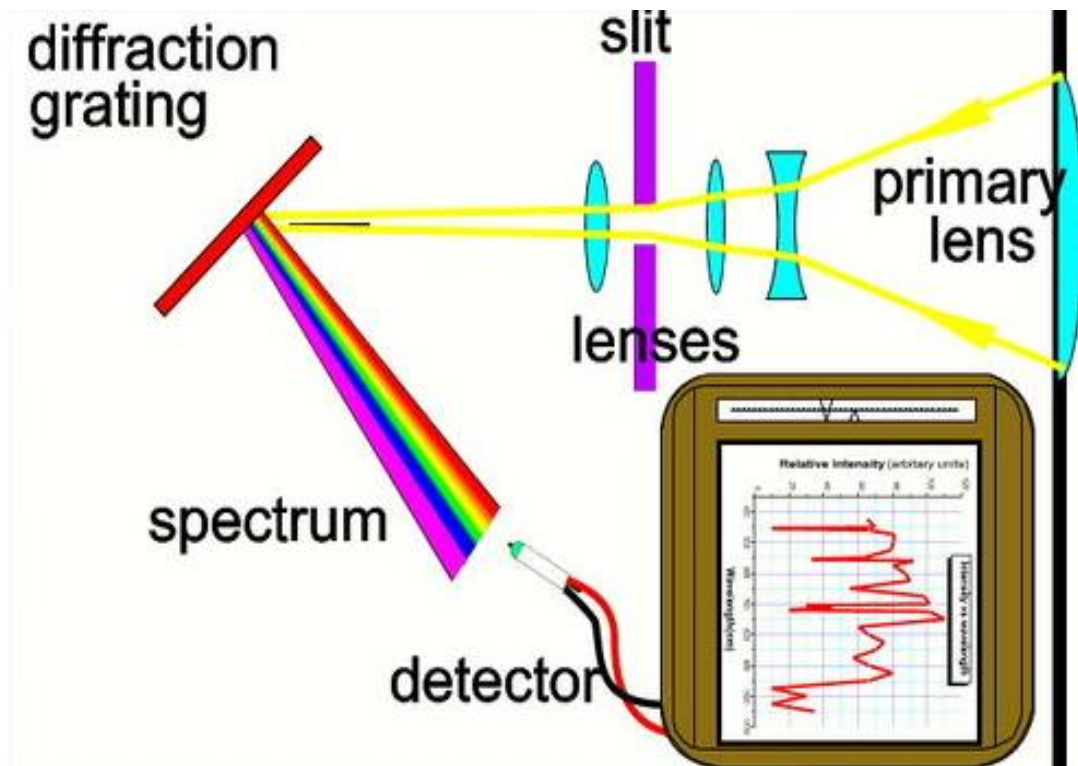


Figure 3: Typical layout of a modern usb powered spectrometer (<http://www.spectralproducts.com/spectrometer>).

With the development in modern CCD image detectors and the advances in computing power available in increasingly small packages, imaging spectroscopy has become a more popular spectroscopy method.

Image spectroscopy is the analysis of the chemical bonds using spectroscopy of spatially determined arrays of positions. An example of this method is the analysis of each pixel of a CCD image sensor. By taking an image of the material whether it is a meteorite, a distant planet, or a length of overhead conductor each position is measured and mapped to show where particular bonds occur in the image.

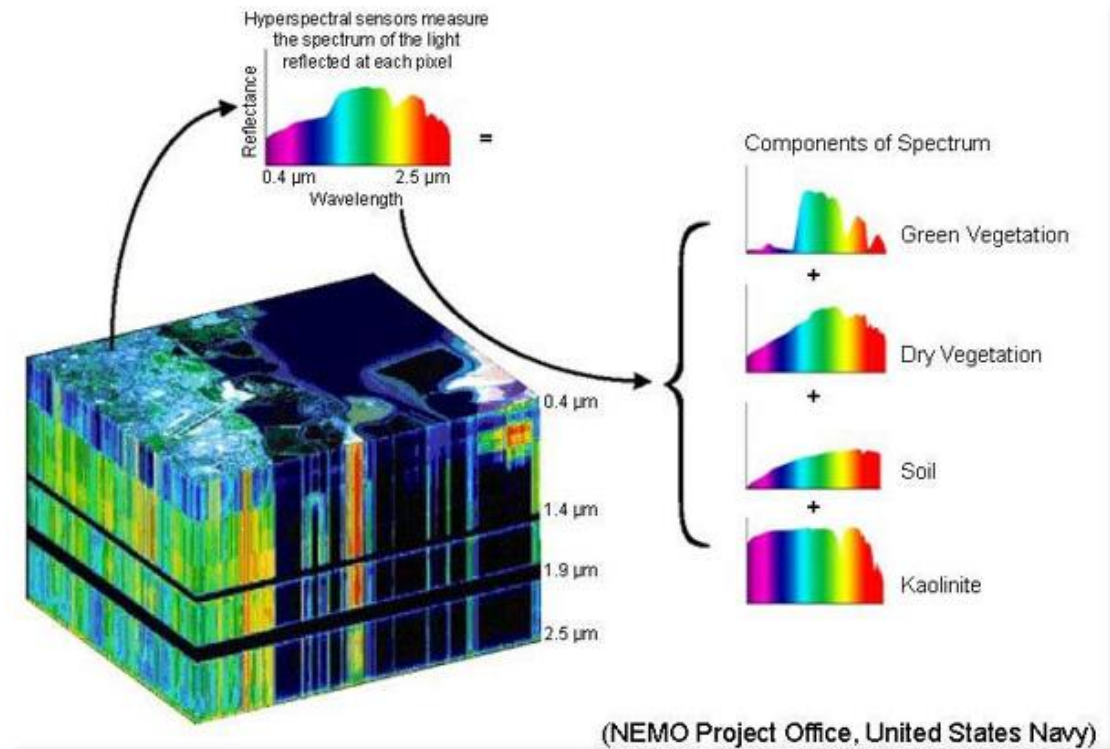


Figure 4: Typical operation of an image spectrometer (Courtesy NEMO Project Office, United States Navy)

The operation of an image spectrometer is essentially the same as a traditional spectrometer but adds a positional component to the measurement, as each pixel is analysed spectrally to determine the materials that make up that part of the image.

Due to its relatively later arrival on the spectroscopy scene, many different terms are being used in conjunction with image spectroscopy some of which are being used in questionable ways. For example the term hyperspectral is being used frequently when describing image spectroscopy. Hyper infers excessive and has occasionally been used to describe the performance of an image spectrometer when the channels measured is in the tens. In modern devices this degree of accuracy of a spectrometer is relatively coarse when compared to the millions of channels employed by a high resolution laboratory spectrometer.

The difference between multispectral and hyperspectral imaging is illustrated in the below figure.

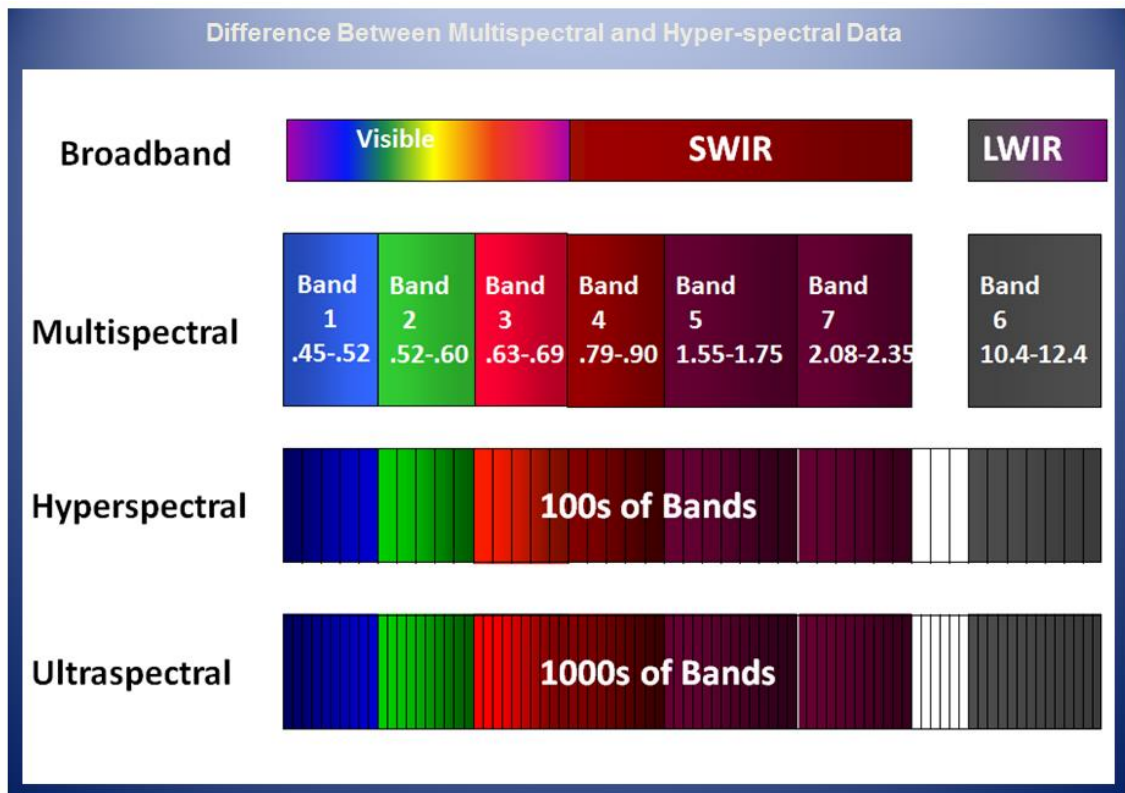


Figure 5: Various spectral measurements by accuracy (<http://www.markelowitz.com/Hyperspectral.html>)

Multispectral imaging is typically used for detecting various materials and objects within a given area and can separate the different elements of the scene into high level classes. A hyperspectral image allows much more detailed classification of the elements such as the health of similar vegetation. Ultraspectral imaging allows quantitative assessment of scene materials such as the abundance of particular gases, or effluents in a particular part of the image.

Modern technology has evolved to allow even sub-pixel fractional abundance of materials using advanced mathematical techniques and allows identification of materials which are smaller than a single pixel in the image captured.

1.3. Project Justification

The environment a power utility in Queensland operates in has changed dramatically in recent times due to a changing political environment and dramatically reduced income as outlined by the AER draft determination (Australian Energy Regulator 2015).

Ergon Energy has responded to this challenge with a dramatic decrease in expenditure which in turn means that all employees are looking for cost effective alternatives to costly solutions

previously proposed. This is no more prevalent than in the engineering ranks as new and innovative solutions are being constantly pursued to solve problems faced.

Conductor material is a primary consideration when tasks such as feeder reviews are undertaken to find any protection reach deficiencies, loading studies are undertaken to identify any capacity or voltage constraints, and copper replacement programs are undertaken to reduce the risk of a conductor failure due to copper deterioration.

There are a very large percentage of conductors on overhead distribution and sub transmission networks which are classified as unknown. This unknown conductor causes many issues for an organisation such as Ergon Energy in the day to day planning and operation of its network. Conductor type is required for the analysis of fault currents, and potential conductor damage in the event of a fault when producing protection settings. Copper conductor is also a major concern on the network as over time the conductor sheds material particularly in coastal environments, this shedding results in a weakening of the conductor and increases the risk of failure and hence increases the risk to the public of grounded conductors. This unknown conductor also results in wasted resources with a large amount of scoping effort required before work is performed on parts of the network with unknown conductor. The identification of conductor material currently requires the use of an uncommonly experienced eye from the ground or very costly physical access which usually involved many hours of planning, isolation and access procedures, customer outage mitigation measures such as generation, and very expensive elevated work platforms.

This project will investigate the use of spectral analysis to remotely identify conductor material. As a quote was obtained for a modern entry level handheld hyperspectral camera (the Bayspec OCI 1000) for \$25,600, a more cost effective method will be used to prove the concept of spectral image analysis. This method includes the use of a Nikon D700 consumer digital SLR camera, a combination of lenses, diffraction gel, the HDR setting on the camera and Matlab to solve the resulting image data cube into a reflectance curve. A commercial plug and play spectrometer will initially be used to test a wide variety of conductors in various states of weathering under a range of lighting levels. The repeatability of these curves will be analysed to make conclusions as to the suitability of spectral analysis for the remote identification of overhead conductor materials.

1.3.1. Current conductor identification methods

Current identification of conductors in the Ergon Energy network is carried out using one technique only. This technique is identification by eye and is a relatively expensive and time consuming method considering the vast network and 1,800 circuit km or 5,400 km of lineal

conductor currently listed as unidentified in the Ergon Energy network. Current state identification is carried out by experienced linesmen or designers as significant skill is required to reliably identify conductor type from the ground. Even experienced resources have difficulty identifying conductor if non ideal conditions are present e.g. cloudy conditions diffusing available light or a sun angle directly behind the conductor make for very challenging conditions as reported by experienced resources. The colour of sun reflection is often the primary method for conductor identification so cloudy conditions which diffuse the available light and prevent a clear reflection from the surface of the conductor present challenges to reliable conductor identification.

In the case of all aluminium and all aluminium alloy conductors there is no method currently employed to differentiate between the two by visual inspection. A method called a “scratch test” is employed where access is gained to the conductor in question and an attempt is made to scratch the surface of the conductor. If the conductor is readily scratched then the conductor is recorded as all aluminium conductor and if the conductor resists the scratching this hardness is assumed to be due to the <1% alloying metal and is recorded as all aluminium alloy conductor. There is considerable costs associated with access to the line as this process usually requires an application to be submitted seven working days in advance, traffic control to be present and a traffic plan submitted to the relevant authority, an elevated work platform to allow access to the conductor, at least three linesman to perform the work, switching to isolate and earth the section of the line to be accessed, and the possibility of an outage to customers.

1.3.2. Cost of current identification methods

In August 2012 Ergon Energy considered a project to identify LV overhead copper conductor in its network. The drive for this project was the “Conductor and Connector Maintenance Refurbishment Strategy” AM-M-STR-0132A which was approved in January 2010. Prior to this project there was a data gathering trial to ascertain the scope of the copper conductor present in the network using asset inspectors to identify copper conductor. Although the experience of the asset inspectors is above average in conductor identification tasks, the trial was a failure and abandoned due to unacceptably inaccurate results. The sole outcome of the trial was an indication that the original cost estimate of \$3.482 M was likely to approach \$20M using similar asset inspection resources due to the training and monitoring that would be required to ensure an accurate result. A second trial was then conducted using highly skilled and specialised design resources to again attempt to identify copper conductor which was successful in providing accurate results.

The deliverables and exclusions for this project were then scoped as:

Deliverables:

- All urban Overhead LV Copper Conductor Data
- Project Schedule, including communications plan
- Review and finalise LV Data Capture process
- Review and finalise LV Data Capture Training
- Deploy process and data capture training
- Development and deployment of Awareness materials to key stakeholders
- IT systems requirements and updates
- Execute data capture program
- Procurement Human Resources, Systems and Tools (8 laptops available)
- Post LV Data Capture Report.
- Project Closure Report.

Exclusions:

- Not identifying LV open points and switches
- Not Identifying LV Fuses
- LV Underground Conductor Data

Again this project was unsuccessful in obtaining endorsement as the estimated \$4,720,471 was considered optimistic and the skills required for conductor identification too hard to obtain. It should be noted that the above project was to identify only LV copper conductor in urban environments (Ergon Energy business case 2010). The lack of available resources with the skills required for this task meant a long and very costly timeline for the project.

1.3.3. Overhead Conductors

1.3.3.1. Common conductor types

Although not exhaustive, a list of the most common conductor types utilised in the Ergon Energy network are as follows:

- AAC 1350 – All Aluminium Conductors
- AAAC 1120 – All Aluminium Alloy 1120 conductors
- AAAC 6201 – All Aluminium Alloy 6201 conductors
- ACSR/GZ 1350 – Aluminium conductors with steel (galvanised) reinforcement
- ACSR/AC 1350 – Aluminium conductors with steel (aluminium clad) reinforcement
- ACSR/AZ 1350 – Aluminium conductors with steel (aluminized) reinforcement
- AACSR/GZ 1120 – Aluminium alloy conductors with steel (galvanised) reinforcement
- AACSR/AC 1120 – Aluminium alloy conductors with steel (aluminium clad) reinforcement
- AACSR/GZ 1120 – Aluminium alloy conductors with steel (galvanised) reinforcement
- AACSR/GZ 6201 – Aluminium alloy conductors with steel (galvanised) reinforcement
- HDBC - Hard drawn bare copper
- HDCC - Hard drawn cad copper
- SC/GZ - Steel conductor (galvanised)
- SC/AC – Steel conductor (aluminium clad)
- ACSR – Smooth body compacted

The following are examples of some standard conductor types at the present time:

- Sub-transmission
 - Oxygen 19/4.75 AAAC 1120
 - Nitrogen 37/3.00 AAAC 1120
 - Iodine 7/4.75 AAAC 1120
- HV Distribution
 - Pluto 19/3.75 AAC
 - Moon 7/4.75 AAC
- HV SWER
 - SCGZ
 - SCAC 3/12 Steel
- LV Mains
 - LV ABC 95 mm²

1.3.3.2. Conductor risk profiles

An advantage of knowing the conductor type and location is that risk due to conductor failure can be identified and managed. One of the tools used to identify the level of risk each

conductor presents is dangerous electrical events (DEE's). Analysis of dangerous electrical events that have occurred in the Ergon Energy network gives some insight into the risk posed by the various conductor types.

An asset related Dangerous Electrical Event is any of the following—

- (a) The coming into existence of circumstances in which a person is not electrically safe, if—
 - (i) The circumstances involve high voltage electrical equipment; and
 - (ii) Despite the coming into existence of the circumstances, the person does not receive a shock or injury;
- (b) The coming into existence of both of the following circumstances—
 - (i) If a person had been at a particular place at a particular time, the person would not have been electrically safe;
 - (ii) The person would not have been electrically safe because of circumstances involving high voltage electrical equipment;
- (c) An event that involves electrical equipment and in which significant property damage is caused directly by electricity or originates from electricity.

Dangerous Electrical Events (DEEs) occur as a result of both assisted and unassisted failure of Ergon Energy's line and substation assets.

Unassisted DEEs are best described as where an asset has failed and the root cause of the failure could have been rectified or identified with a maintenance methodology. For example: Corrosion, rot decay, termites, leakage, vibration and mechanical failure.

Assisted DEEs are best described as where the root cause of the failure occurs outside the control of the maintenance regime and the asset was operating within specifications. For example: Storm, fire, lightning, vegetation and vehicle impact.

The vast majority of DEEs occur on the overhead network, and conductor and connector failure can have severe consequences for staff and public safety, as well as serious reliability impacts and the possibility of environmental damage.

Although no specific targets are enforced for the number of DEEs experienced each year, Ergon Energy has a strong focus on reducing the number of DEEs to as low a level as reasonably practical. As a minimum, Ergon Energy is focussed on keeping DEEs in the realms of historical averages.

The only regulatory target related to asset performance is the Pole Reliability Performance Target of 99.99% contained within the Code of Practice - Works, QLD Electrical Safety Act 2002. Ergon Energy is presently exceeding this target with 99.996% reliability.

DEE events can have an adverse effect on the performance and reliability of the network as these events can result in network outages, which inconvenience customers and reduce revenues. This also affects MSS and STPIS targets. The benefits of complying with or exceeding these targets include an improved perception of Ergon Energy by our customers, compliance with license requirements and financial benefits.

The annual total number of asset related Dangerous Electrical Events (DEEs) is difficult to predict, however having an understanding of the types and causes of DEEs, analysis can be performed to highlight areas where efforts should be focused or targets reviewed and changed as appropriate.

An analysis of DEEs revealed that conductors represent the asset class with the highest number of incidents. Figure 2 shows DEE performance for the most recent financial year. It is clear from this figure the substantial impact conductor performance has on overall DEE results. It can be seen conductor is responsible for the highest number of assisted DEEs, and the second highest number of unassisted DEEs.

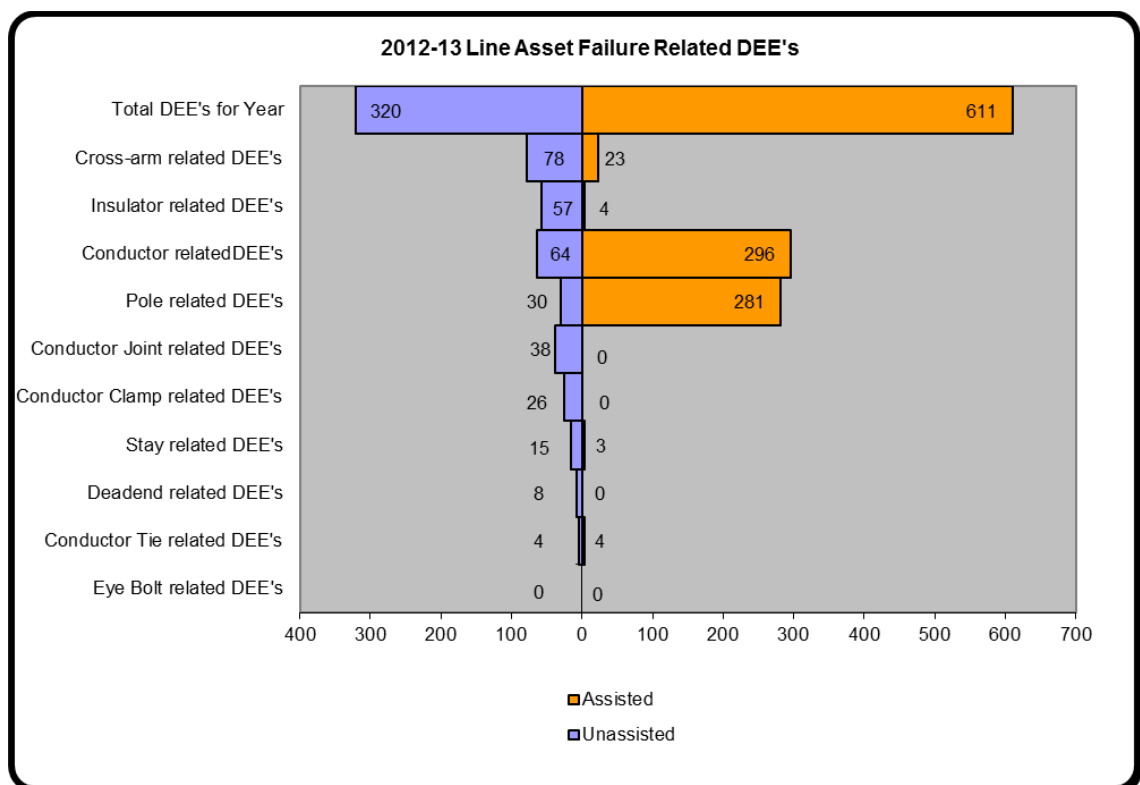


Figure 6: Top five P2 conductor defects trended over time

The following figure of conductor P1 defects shows clearly that there are 5 major conductor types which create the majority of conductor defects. These are:

- Bare Aluminium Conductor

- Bare Steel Conductor
- LV Covered Conductor
- Bare Copper Conductor
- LV ABC

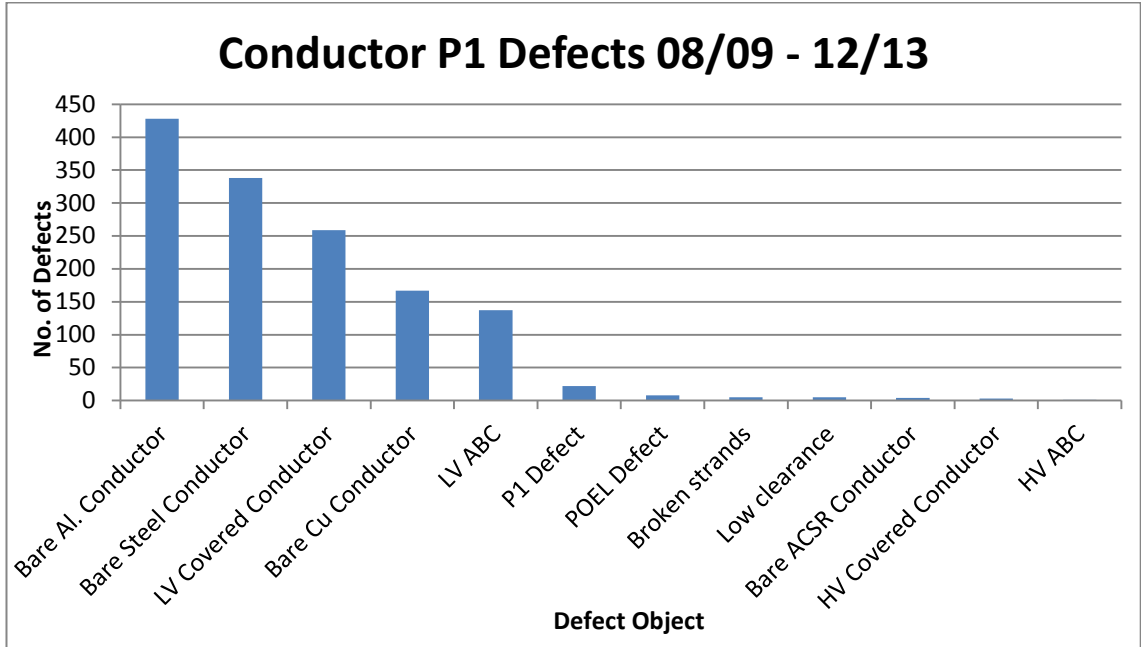


Figure 7: Conductor P1 defects 08/09 – 12/13

These same 5 types are responsible for the significant majority of P2 Defects.

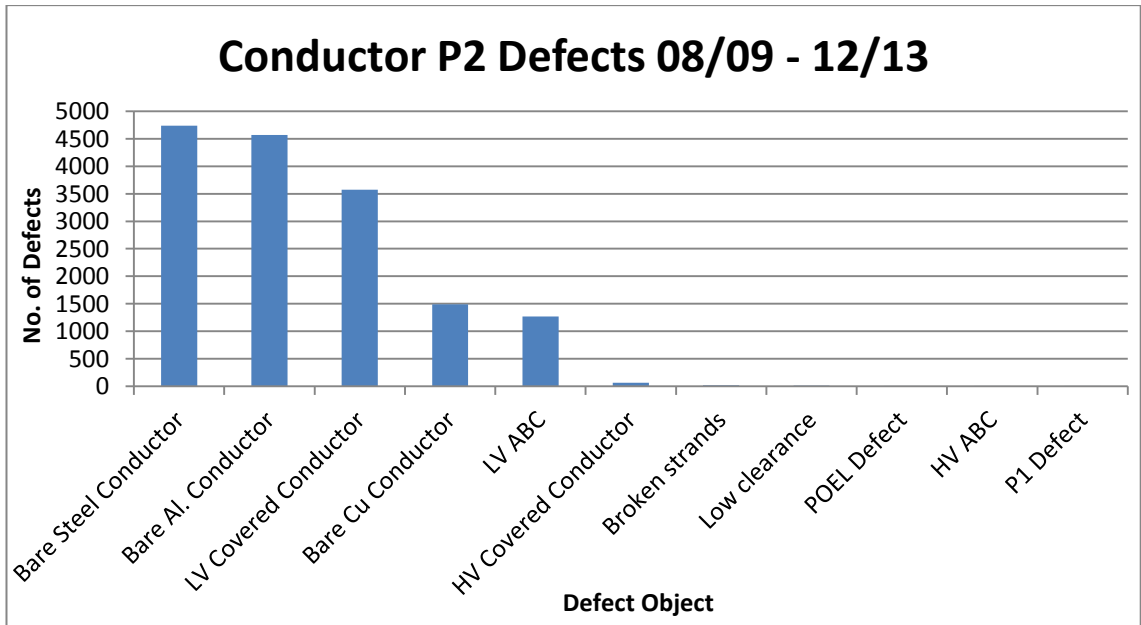


Figure 8: Conductor P2 Defects 08/09 – 12/13

Trended over time, it is clear to see that all 5 conductor types have experienced an increase in P2 defects since 2008/09.

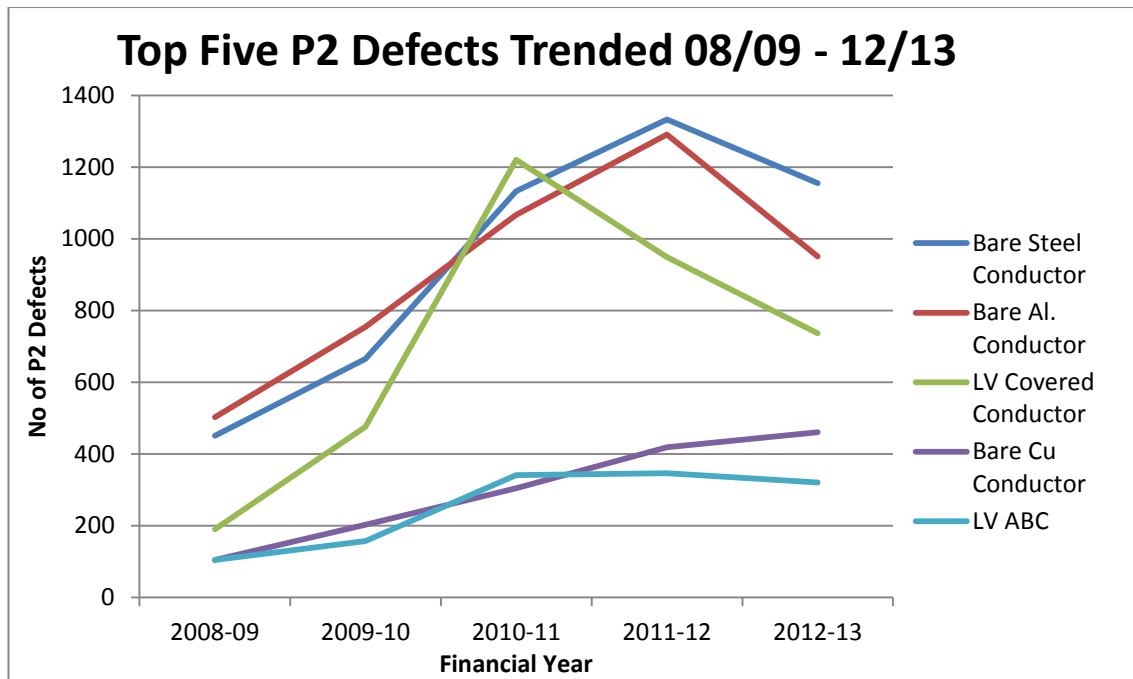


Figure 9: Top five P2 conductor defects trended over time

Closer analysis into the damage description of these defects allows for more detailed examination of the real cause of these defects. A trend in the damage description is quite obvious, with all conductors showing the same top 6 damage descriptions.

Ergon Energy is currently performing replacements of aged and deteriorated small diameter copper conductor in high risk locations. This is a gradual program which seems to have been occurring sporadically as necessary by the Regional Asset Management (RAM) teams and mainly consists of copper conductor replacements. A risk criterion for this work has been developed by the RAM teams and managed locally.

As identified previously in this strategy document, there are currently significant data gaps on the quantity, age, condition and location of both conductors and connectors – especially LV conductor. Data exists in Ergon Energy’s GIS system, however the conductor type in particular has not been found to be accurate, resulting in a requirement for on-site scoping work prior to any project work. Effort has been made to develop an assumption-based model of subtransmission and HV distribution conductors via the CBRM process, but this uses corporate system data and is therefore affected by inaccuracies also. These models are currently incomplete.

Ergon Energy was formed from 6 regional corporations and as a result has a variety of voltages and equipment types.

Most of Queensland is considered a harsh environment consisting of:

- High rainfall in the wet tropical north and some of the other coastal areas.
- High level of corrosion due to salt laden atmosphere in coastal areas and localised industrial pollutants in some areas (eg Gladstone and Yabulu).
- Abnormally high lightning activity particularly in western areas.

Ergon Energy has inherited overhead lines comprised of many different conductors and connectors.

A significant population of line assets were constructed prior to 1960 and whereas the poles have been inspected and reinstated as a routine process and some lines completely reconstructed, there are significant quantities of conductor which is now over 50 years old. The predominant conductor of concern is small diameter hard drawn bare copper (HDBC) which has performed very well but now presents a variety of risks to the business.

Conductor materials have changed over time with older conductors tending to be hard drawn bare copper (HDBC). This was superseded by all aluminium and aluminium conductor steel reinforced (AAC and ACSR). Whilst these aluminium conductors are still used all aluminium alloy conductors (AAAC) have been increasing in popularity during recent years.

The conductor type used potentially presents the following problems:

Copper conductor:

Aged HDBC suffers from:

Work hardening

Annealing (often from burning of sugar cane and faults)

Corrosion and scale (from exposure to coastal elements)

Splatter damage (from conductor clashing)

Mechanical failure (from bird strikes and vegetation)

Poor reliability due to failures causing customer outages

May have insufficient fault rating

Small HDBC distribution conductors (eg 7/.064 and 7/.080) are an identified risk due to their small diameter. This has been exacerbated by the build-up of scale, making the conductor appear 'solid' when in fact it is substantially corroded away once the scale is removed.

Steel conductor:

Some issues with rusty 3/2.75 SC/GZ steel conductor particularly due to corrosive coastal environments have been identified. However, at this stage, it is unclear how much impact rusting has on the structural integrity and current carrying capacity of the conductor.

Burning of sugar cane causes considerable conductor damage leading to failure.

Damage to the coating on Steel conductors leading to corrosion (rust)

Electrical losses in steel conductors in SWER systems

Vibration damage

Often has insufficient fault rating (protection issue)

Aluminium conductor (including ACSR)

Burning of sugar cane causes considerable conductor damage leading to failure:

Softening of Aluminium conductors

Oxidisation of aluminium

Oxidisation is more likely in coastal zones (close to the coast).

Occasional issue with ACSR conductors.

Vibration issues in open plain areas.

The age and condition of conductor presents significant challenges for Ergon Energy. This strategy represents a structured approach to try to understand conductor condition and the development of holistic strategies or solutions.

1.4. Project Objectives

Although representing the potential for relatively inexpensive, and timely conductor identification, the use of spectral analysis is unlikely to become common practise if conductor material identification is not accurate or consistent. On this basis the main objectives of the project are to:

1. Research conductor metallurgy to identify the composite metals that make up commonly used overhead conductors.
2. Critically evaluate current conductor identification techniques.
3. Evaluate spectroscopy as a method of identifying overhead conductor materials under laboratory conditions.
4. Attempt the construction of an image spectrometer using a consumer camera to further understanding and test the device on a conductor sample.
5. Submit an academic dissertation on the research.

If time permits there are further objective that would be desirable to achieve:

1. Evaluate methods of remote conductor diameter measurement to use in conjunction with hyper spectral analysis to definitively identify overhead conductor.
2. Investigate the feasibility of integrating conductor material identification and diameter measurement into the ROAMES LiDAR aircraft which overflies the entire Ergon Energy network each year.

1.5. Chapter Overview

The following gives a brief chapter overview:

Chapter 1 – Introduction: Presented an overview of the facets of the project and investigated the various conductor types present in the Ergon Energy network.

Chapter 2 – Literature Review: Presents the literature concerning spectroscopy and in particular the factors that influence the measurement of spectral curves, the quality criteria applied to spectroscopy, an inexpensive means of producing an image spectrometer, and the various conductor types present in the Ergon Energy network.

Chapter 3 – Methodology: Outlines the approach to fulfilling the project objectives including the use of a commercial usb plug and play spectrometer followed by an attempt to produce an inexpensive image spectrometer, and further testing using this device.

Chapter 4 – Results and Discussion: An assessment of the results of the spectral measurements and a discussion on the outcome.

Chapter 5 – Conclusion and Recommendations: An assessment on the success in achieving of the objectives and an outline of the findings including identification of opportunities for further research.

1.6. Limitations & Restrictions

The following limitations and restrictions apply to the project and dissertation:

. The project is limited to the consideration of the following conductors:

- All Aluminium Conductor (AAC)
- All Aluminium Alloy Conductor (AAAC)
- Hard Drawn Copper Conductor (HDDB)
- Galvanised Steel Conductor (SC/GZ)

To comply with confidentiality and security restrictions, locations will not be revealed when discussing conductor types.

1.7. Chapter Summary

This chapter has provided a brief background and an introduction to the dissertation. Firstly, an overview of spectroscopy was discussed to provide a more detailed understanding of the results of the measurements and the factors which may have influenced the results. The past trend in increasing electricity prices and the recent measures implemented by the Australian Energy Regulator was also discussed. This provided essential background information necessary for fully appreciating the need for the study which was presented next. The need for the project was explained by presenting a recent Ergon Energy business case to identify a small cross section of conductor and the prohibitive cost estimated to carry out the project. The risk presented by various conductor types also provided justification for the need to identify conductor types. The introduction chapter concluded with a statement of the project objectives, limitations and restrictions; and a brief overview of each chapter.

2. Literature Review

2.1. Chapter Overview

The aim of this project stated in chapter 1 is to gain an understanding of spectroscopy as a method of remotely identifying conductor materials on the Ergon Energy overhead network by studying the associated literature. To enable a greater understanding it is clear that a detailed understanding of spectroscopy is required. This chapter outlines the research results on both the proof of concept image spectroscopy, and spectroscopy performed using a commercial plug and play usb spectrometer. The literature review will investigate many facets of this project and will specifically achieve the first objective of this project:

1. Research conductor metallurgy to identify the composite metals that make up commonly used overhead conductors.

2.2. Reflectance transmittance emittance and absorption.

As photons enter a material and encounter the particles that make up that material, they are reflected or refracted. It is useful to investigate these processes to more fully understand the mechanics of spectroscopy. As part of this project we will need to measure the reflected light wave and all materials have a complex index of refraction which may be described by the formula (Hecht 2001):

$$m = n - jK \quad (2.1)$$

Where K is the imaginary part of the index or refraction, referred to as an extinction coefficient, m is the complex index of refraction, and n is the real part of the index ($j = -1^{1/2}$)

As the photons enter an absorbing medium, they are absorbed in a manner that can be described by Beers Law:

$$I = I_0 e^{-kx} \quad (2.2)$$

Where I is the observed intensity, I_0 is the original intensity, x is the distance travelled through the medium, and k is the absorption coefficient (Hecht 2001). Absorption coefficients are usually expressed in units of cm^{-1} and x is expressed in cm. The above formula is accurate for a single wavelength, as the wavelength varies so too does the absorption coefficient and the index of refraction. At visible and near-infrared wavelengths the index of refraction generally varies less than the absorption coefficient as a function of wavelength. The wavelength where $n=1$ is called the Christensen frequency and is usually the point where reflected light is at a

minimum. This is due to the small difference in the index of refraction when compared to the surrounding environment.

Fresnel (1819) also described the behaviour of light wave travelling with a velocity V in a medium with relative permittivity ϵ_r , the light intensity I can be described in terms of the electric field amplitude E_o (Kasap 2001):

$$I = \frac{1}{2} \epsilon_r \epsilon_0 E_o^2 \quad (2.3)$$

Where $\frac{1}{2} \epsilon_r \epsilon_0 E_o^2$ represents the energy in the field per unit volume. When we multiply this energy by the velocity v we calculate the rate at which energy is transferred through a unit area, and as $v = c/n$ and $\epsilon_r = n^2$ the intensity is proportional to nE_o^2 .

Fresnel (1819) described reflectance in a way that measures the intensity of the reflected light with respect to the incident light and can be defined separately for parallel and perpendicular incidences to the plane of incidence. If the perpendicular component is R_{\perp} and the parallel component is R_{\parallel} then the formulae for each component is given as:

$$R_{\perp} = \frac{(E_{ro,\perp})^2}{(E_{io,\perp})^2} = (r_{\perp})^2 \quad (2.4)$$

And

$$R_{\parallel} = \frac{(E_{ro,\parallel})^2}{(E_{io,\parallel})^2} = (r_{\parallel})^2 \quad (2.5)$$

When light is reflected the phase of the light may be changed resulting in a reflection coefficient as a complex number, the actual reflectance is represented by intensity changes (mostly percentage) so are necessarily real numbers. For example when $(E_{ro,\parallel})^2$ is a complex number then:

$$(E_{ro,\parallel})^2 = (E_{ro,\parallel})(E_{ro,\parallel})^* \quad (2.6)$$

Where $(E_{ro,\parallel})^*$ is the complex conjugate of $(E_{ro,\parallel})$

Therefore in the case of a normal incidence the reflectance is given by:

$$R = R_{\perp} = R_{\parallel} = \left(\frac{n_1 - n_2}{n_1 + n_2} \right)^2 \quad (2.7)$$

As an example glass has a refractive index of around 1.5 which will mean that around 4% of the incident light striking the glass/air surface will be reflected back.

In a similar vein Fresnel (1819) described transmittance as the intensity of the transmitted wave to that of the incident wave. When considering transmittance we must take into account the fact that the light wave has been diffracted and is therefore travelling at a different angle to the boundary and is travelling in a different medium. For normal incidence the incident and transmitted beams are normal and the transmittances can be described by the equation:

$$T_{\perp} = \frac{n_2(E_{t0,\perp})^2}{n_1(E_{i0,\perp})^2} = \left(\frac{n_2}{n_1}\right) t_{\perp}^2 \quad (2.7)$$

And

$$T_{\parallel} = \frac{n_2(E_{t0,\parallel})^2}{n_1(E_{i0,\parallel})^2} = \left(\frac{n_2}{n_1}\right) t_{\parallel}^2 \quad (2.8)$$

In normal laboratory conditions emittance can usually be ignored simply because the subject can be lit with enough light to create a reflectance large enough to make any emittance insignificant. Ideally conductors would be measured remotely with no requirement for an external light source so emittance cannot be ignored in this case. As stated above all material emit energy unless cooled to absolute zero biasing any reflectance measurements. Kirchofs Law (Nicodemus 1977) can be used to find a value for emissivity and can therefore be accounted for in any measurements. Kirchofs Law states:

$$E = 1 - R \quad (2.9)$$

Where E is the emissivity, and has been proven to be accurate to a satisfactory standard (Salisbury 1998). Although some inconsistencies have been found while using the law (Duggin & Philipson 1982) these can generally be attributed to a requirement for critically accurate results and may be due to temperature gradients in the subject. For the purpose of this study inconsistencies in the material grain size will produce much larger spectral changes than any slight departure from the model.

2.3. Factors affecting spectral reflectance measurements.

There are a variety of factors which affect the repeatability and accuracy of spectral reflectance measurements. Much previous research has identified these issues and includes atmospheric properties, the time, height, and orientation of the measurement, and the field of view and calibration of the measuring device (Nicodemus 1977; Duggin & Philipson 1982; Milton 1987; Curtiss & Goetz 2001; Milton, Rollin & Emery 1995; Jupp 1997; Salisbury 1998; Schaeppman 1998).

Accurate spectral measurements are required for many applications including the calibration of satellite sensors (Slater et al. 1987) and atmospheric correction (Moran et al. 2001). Field spectroscopy is commonly used for this purpose and is usually a ‘single-beam’ method which involves sequential measurements of the spectral radiance from the target followed by a measurement of a calibrated reference panel (Milton 1987). To understand the factors affecting spectral reflectance it is useful to first understand what reflectance is actually measuring.

Spectral radiance is very useful when taking measurements using a spectroradiometer and is useful in measuring the directional effects of the radiation. The radiance returned is entirely dependent on the incident radiation used to light the surface. Reflectance is therefore defined as the ratio of reflected flux to incident flux and is expressed in percentage terms.

Due to the presence of a limited light source and field of view of the measuring device the measurement of reflectance is carried out in a field which is conical or hemispherical in shape. If we take the example of reflectance measurements being taken in the field, the light source is the sun however the actual irradiance reflected from the sample can be divided into the direct sunlight component and a second more diffuse or anisotropic light which reaches the sample after being scattered by the terrain, and atmospheric conditions such as pollutants and clouds. The ratio of the diffuse and direct components can have a significant effect on the results (Nicodemus 1977).

As diffuse components are always present when in the field due to the scattering effects of topology, atmospheric conditions, the surfaces surrounding the object being measured, and the wavelength of the light, it is of the utmost importance to use the correct measuring device to minimise these effects (Schaepman-Strub et al. 2006). Many unexpected results can be attributed to a lack of consideration for the illumination (including the diffuse component), and the viewing geometry including the opening angle.

The directional/anisotropic hemispherical reflectance factor (Gu and Guyot, 1993). $R(0^\circ/h^*)$ is calculated as:

$$R(0^\circ/h^*)_\lambda = \left(\frac{L_\lambda}{LP_\lambda}\right) Rp(0^\circ/h^*)_\lambda \quad (2.10)$$

Where L_λ is the flux from the surface, LP_λ is the flux from the reference panel, $Rp(0^\circ/h^*)_\lambda$ is the directional/anisotropic hemispherical reflectance of the reference panel which is measured under the same conditions (viewing geometry and illumination) as the surface. $R(0^\circ/h^*)_\lambda$ is therefore an approximation of the true bidirectional reflectance factor of the surface as the

instrument field of view and haze present in the atmosphere has an impact on the measurement.

For the purpose of this research emphasis is placed on the precision of the results where precision implies results can be repeated with similar results. The accuracy of the results (which refers to the correlation between the measurement and some recognised standard) is not particularly helpful in this research as very little previous measurement and analysis has been undertaken on the spectral response of the materials in use as overhead conductors. This being the case, part of the further work to be undertaken not in the scope of this dissertation is the creation of a spectral library of overhead conductors against which field results can be compared to identify materials.

The issues to be considered when creating such a spectral library cannot be found in any single document or place and include:

- The environment including
 - Wind speed and direction
 - Cloud cover and type
 - Temperature and humidity
 - Aerosols in the atmosphere
- The viewing geometry including
 - The field of view of the measuring device
 - The distance from the sample to be measured
- The illumination conditions including
 - The sun altitude, azimuth and orientation
 - The presence of smoke and haze
- The properties of the sample including
 - The surface texture of the sample
 - The chemical and structural makeup of the sample

When obtaining spectral imaging from height either satellite or aircraft the atmospheric effects on remote sensing imagery can cause a scattering of the light which will cause a loss in the finer details of the image. Steps must be taken to correct for these atmospheric effects particularly when there is a high degree of detail in the image such as attempting to identify overhead conductors in an urban environment. These atmospheric effects become particularly troublesome when measurements are taken from height with a wide angle sensor as there will be a much greater atmospheric path length in the extremities of the field of view than in the centre resulting in a non linear effect to be accounted for. These atmospheric effects are also

inconsistent across the range of bandwidths with the 0.5 to 0.6 μm spectrum of the colour green being affected much more than the longest infrared band of 0.8 to 1.1 μm (Richards & Xiuping 1998).

Another source of error in spectral imaging measurements is radiometric errors within a band and between bands. The response of a particular band in the sensing instrument ideally would be linear, however modern detectors will all have some degree of error creating a drift of the ratio of signal to response. As these errors differ from band to band the output from one band may drift into the adjacent band creating a severe error that can render the image unusable. Similarly equipment that is operated above absolute zero will have some background noise creating an offset historically known as dark current.

As spectral imaging records a spatial component and often records the image from a satellite or other significant height from the object to be measured geometric distortion is also a source of error. These geometric errors may include:

- The rotation of the earth during image acquisition
- The finite scan rate of some sensors
- The wide field of view of some sensors
- The curvature of the earth
- Sensor non-idealities
- Variations in sensor altitude, attitude and velocity
- Panoramic effects related to the imaging geometry

2.4. Quality criteria for reflectance measurements.

There are three criteria which can be used to assess spectral reflectance measurements. These three elements are traceability, repeatability and reproducibility (Fox 2001). Traceability is a continuous chain of comparisons, each with uncertainty, which links a measurement to a recognised standard. The magnitude of the uncertainty is dependent on the reference panel used and the stability and linearity of the spectrometer used.

Repeatability refers to the spread of the results of successive measurements of the same sample carried out under the same conditions.

A measure of the strength of correlation between the measurements of a certain conductor type is the correlation coefficient of the data sets (Snedecor & Cochran 1980). The correlation coefficient is a measure of the strength and direction of the linear relationship between two variables and provides an indication of the strength of the correlation between two or more sets of variables and is sometimes referred to as the Pearson product moment correlation

coefficient. If for example we have two variables X and Y and a sample size of N the correlation coefficient (r) is represented by:

$$r = \frac{N \sum XY - (\sum X)(\sum Y)}{\sqrt{N(\sum X^2) - (\sum X)^2} \sqrt{N(\sum Y^2) - (\sum Y)^2}} \quad (2.11)$$

Where N is the total of the pairs of data points. Or in the case of the excel "CORREL" function in Microsoft Excel:

$$\text{Correl}(X, Y) = \frac{\sum(X - \bar{X})(Y - \bar{Y})}{\sqrt{\sum(X - \bar{X})^2} \sqrt{\sum(Y - \bar{Y})^2}} \quad (2.12)$$

Where \bar{X} and \bar{Y} are the sample means of the two arrays of data.

The total range of r is +1 to -1 with the positive and negative signs differentiating between positive linear correlation and negative linear correlation respectively. If there is a strong positive correlation i.e. there is a strong relationship between the X and Y movement in the same direction, the correlation coefficient (r) will be close to +1. Conversely if there is a strong negative correlation there will be a strong relationship between the X and Y movement in the opposite direction, the correlation coefficient (r) will be close to -1. If there is little or no linear correlation the correlation coefficient will be closer to 0 which indicates a random, non linear relationship between the two variables X and Y .

There can only be a perfect negative or positive correlation coefficient if all data points lie on a perfectly straight line. If $r=+1$ then the slope of this line will be positive and if $r=-1$ then the slope of the line will be negative. A correlation coefficient greater than 0.8 is generally described as a strong correlation, and a correlation coefficient less than 0.5 is generally described as a weak correlation.

2.5. Analysis of an inexpensive means of spectral photography as proof of concept

Conductor material is a primary consideration when tasks such as feeder reviews are undertaken to find any protection reach deficiencies, loading studies are undertaken to identify any capacity or voltage constraints, and copper replacement programs are undertaken to reduce the risk of a conductor failure due to copper deterioration.

Spectral imaging is a very well researched and understood topic. The spectral output of satellite or aircraft mounted systems has been used extensively in the mapping of geological and mineralogical features for some time (Clark 1999) and has distinct advantages over conventional lower resolution spectral imaging in that materials can actually be identified

when compared against known spectral reflectance curves rather than just separated as different.

Spectral imaging has however traditionally been confined to mining and other geological uses due to the cost of these systems and have been mounted in aircraft or satellites. Field based applications of this form of imaging have not been fully explored and have certainly never been used to identify overhead conductor materials.

The foremost requirement for successful spectroscopy image is that a large amount of light must be gathered to include enough information from each spectrum to provide a reliable and repeatable spectral curve for analysis. This is usually achieved through the use of diffraction gratings, and very large optical elements including very specialized sensors. The common use of high dynamic range (HDR) imaging in modern high end consumer cameras can provide the necessary volume of light by combining many images of the same scene at different exposures and combining them to create a single image of much greater dynamic range than would be achievable with a single exposure. Instead of a highly specialised monochromatic sensor to capture the spectral data we can instead use the much simpler Bayer filter array present in a consumer camera.

Okamoto (1993) has paved the way for the use of higher end consumer cameras manufacturers meaning that Image Spectroscopy technology is now achievable by modifications to a high end consumer camera such as the Nikon D700 and a relaxation of any requirement for sub second exposure times. The camera is used to capture a HDR image in the form of a data cube which must be then mathematically solved to produce a spectral curve which may be matched with known curves of materials. This method has some disadvantages in longer exposure times and the requirement for some post processing with Matlab, but makes the use of spectral photography within the means of anyone with a higher end camera capable of HDR image capture.

The capturing of the three dimensional spectral data cube can be achieved by a number of different methods. The primary difference in these methods is the way in which they separate the incident light in the different spectral components. The methods used to achieve this are using dispersive elements, diffractive media or changeable/tuneable bandpass filters (Harvey 2000). Du et al. have investigated the use of a standard prism/slit configuration array but this approach results in a large file with relatively poor resolution. Another approach uses spectrally separate light sources one after the other to light the subject and combine the images. This method is unreliable as changes in the ambient lighting conditions vary the results.

The most suitable method appears to be computed tomography imaging spectrometry. This method diffracts the spectral elements spatially by projecting the 3D data at varying angles onto the image sensor. This image can then be reconstructed by inverting the projection. Computed tomography imaging spectrometry (CTIS) avoids the problems introduced when a traditional dynamic scanning of the scene is carried out such as movement due to long scan times, and the moving parts traditionally employed by these scanners. CTIS technology is already relatively mature due to its use in all the above mentioned applications such as biomedical, military, and space observation.

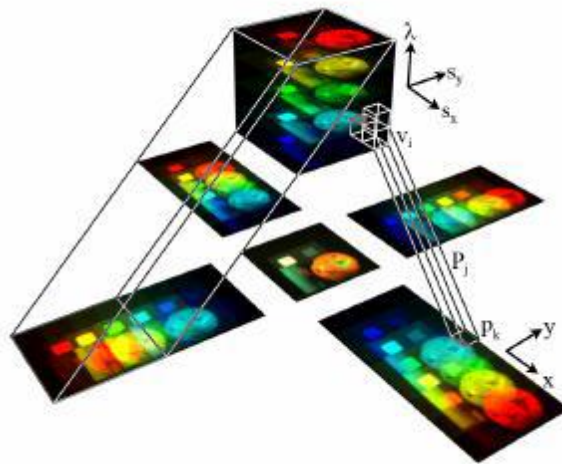


Figure 10: Creating parallel projections by diffracting the image (CTIS)

Although no literature was found which uses this method to identify overhead conductor materials, Image Spectroscopy is currently used for tasks such as identifying objects in space (Hege et al. 2003), identifying cancerous growths (Johnson et al. 2007) and the finding mines by military surveillance (Descour, Derenia & Dubey 1995) so the task of identifying a relatively pure metallurgical element from the ground with the sky as a background should provide a strong match to a known library of elements.

The capturing of the three dimensional spectral data cube can be achieved by a number of different methods. The primary difference in these methods is the way in which they separate the incident light in the different spectral components. The methods used to achieve this are using

dispersive elements, diffractive media or changeable/tuneable band pass filters (Harvey et al. 2000). Du et al. have investigated the use of a standard prism/slit configuration array but this approach results in a large file with relatively poor resolution. Another approach uses spectrally separate light sources one after the other to light the subject and combine the

images. This method is unreliable as changes in the ambient lighting conditions vary the results.

The most suitable method appears to be computed tomography imaging spectrometry. This method diffracts the spectral elements spatially by projecting the 3D data at varying angles onto the image sensor. This image can then be reconstructed by inverting the projection. Computed tomography imaging spectrometry (CTIS) avoids the problems introduced when a traditional dynamic scanning of the scene is carried out such as movement due to long scan times, and the moving parts traditionally employed by these scanners. CTIS technology is already relatively mature due to its use in all the above mentioned applications such as biomedical, military, and space observation.

2.5.1. CTIS and Fourier Transformation of the Image Data.

The use of Matlab to perform the calculation intense transformation of the data cube the camera produces to a reflectance curve would seem like a natural fit but was only pioneered by Hagan (2007) who suggested the use of Fourier series and multithreading to reduce the processing time dramatically to allow timely solutions of the data cube using readily available software and desktop hardware.

Traditionally the very high computational demands of computed tomographic image spectroscopy have been a very discouraging barrier to a more widespread use of the technology. The rapid increase in processor speed, the increase in cores available in each processor commonly used in consumer level computers, and the advancements made in applications such as Matlab to more efficiently utilise these cores have enabled a new approach toward resolving the required data cubes for CTIS.

A novel approach was presented by Hagen (2007) which uses a spatial shift-invariance to greatly reduce the dimensionality of the matrix inversion process required in the reconstruction of the data cube. Hagen (2007) claims an increase in the speed of the data cube reconstruction in the order of 4000.

CTIS is a method of acquiring a cube of data which contains the spectral measurement of a particular scene. This is achieved with the use of a dispersive element which breaks the light photons up into its constituent frequencies (for the purposes of this project that is a diffraction gel). A field stop to limit the field of view and prevents the direction orders from overlapping is also used and in this case was achieved with the use of a square aperture. The combination of the diffraction grating and the field stop square aperture creates a set of prismatically splayed streaks, each one of which contains the spectral measurement of the scene.

The traditional method to reconstruct the datacube from the measured image is to use a linear imaging equation.

$$g = H \cdot f(x, y, \lambda) \quad (2.13)$$

Where g is the image (output), H is the system operator, and f is the object or input. If we were to place the pixel information of the measured image into a single one dimensional vector lexicographically (i.e. when applied to subsets, two subsets are ordered by their smallest elements. For example, the subsets of $\{1, 2, 3\}$ in lexicographic order are $\{\}, \{1\}, \{1, 2\}, \{1, 2, 3\}, \{1, 3\}, \{2\}, \{2, 3\}, \{3\}$.) indexed by m and do the same for each voxel (position in three dimensions) in the datacube (indexed by n) then each element H_{mn} of the system matrix maps the sensitivity of voxel f_n in the datacube to a pixel g_m in the image. This traditional method continues as described by Hagen(2007) where an object f from measured image g requires inversion. Two iterative reconstruction algorithms based on the expectation maximisation (EM) method or the multiplicative algebraic reconstruction technique (MART).

$$EM: \hat{f}^{(k+1)} = \frac{\hat{f}^k}{\sum_{m=1}^M H_{mn}} \left(H^T \frac{g}{H \hat{f}^k} \right) \quad (2.14)$$

$$MART: \hat{f}^{(k+1)} = \hat{f}^k \left(\frac{H^T g}{H^T H \hat{f}^k} \right) \quad (2.15)$$

Where \hat{f} is an estimate of the objects datacube and the k superscript is the iteration number. Although algorithms exist which eliminate the zero values in the matrices to be computed, the resulting calculation still requires approximately 5×10^{10} floating point calculations which could take a modern desktop computer anywhere from 10 minutes to an hour to complete.

As the above method does not provide the required calculations in a timely enough manner alternative approaches must be investigated. The method chosen makes use of the knowledge that the CTIS system matrix is spatially shift-invariant to improve the reconstruction algorithms. A characteristic of a spatially shift-invariant matrix is that it can be diagonalized by Fourier transformation. This means that the H matrix can be diagonalized along its spatial dimensions using a Fourier transformation which should reduce computing time dramatically.

To fully understand how to apply Fourier transformation to the diagonalizing of the spatial dimensions when using CTIS, it is useful to imagine the CTIS system as a deck of cards. As can be visualized in the below figure the discrete slices of the data cube of which there are L number of monochromatic images indexed by ℓ and $(1 \leq \ell \leq L)$. Using this setup we then have:

$$h(r, r_d, \lambda_\ell) \equiv h_\ell(r - r_d) \quad (2.16)$$

This formula implies that each wavelength λ_ℓ has a convolution kernel h_ℓ which describes the object to image mapping. This imaging equation when converted to the frequency domain, resolves to:

$$G_\ell(p_d) = k_\ell(p_d)F_\ell(p_d) \quad (2.17)$$

This formula reduces the full CTIS matrix multiplication issue into L sub-multiplications. Each of these sub-multiplications is diagonal. The traditional approach to matrix – vector multiplication above required 5×10^{10} floating point calculations whereas this new approach using $G_\ell(p_d) = k_\ell(p_d)F_\ell(p_d)$ will result in $100 \times 100 = 10\,000$ operations at each of the 600 wavelengths for a total of approximately 12×10^6 flops which is a large reduction.

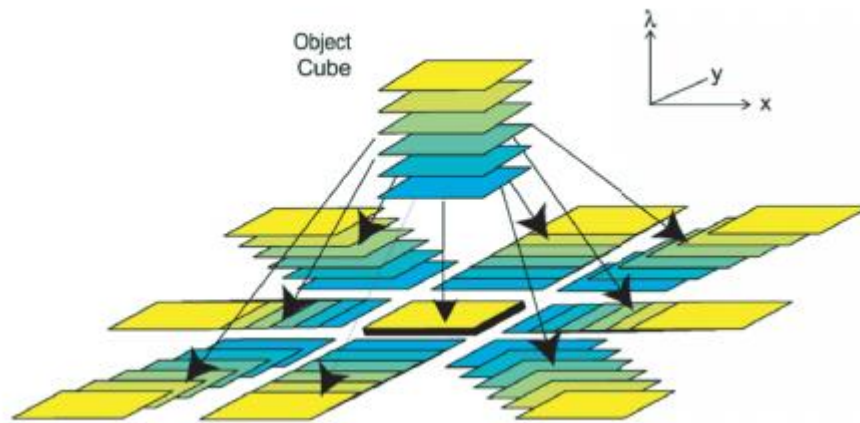


Figure 11: Representation of the CTIS image cube and deck of cards analogy (Hagen, Dereniak & Sass 2007).

Although the above theory is sound, Hagen (2007) describes a problem in the application. While measuring H during calibration, we actually need to use K in the domain for the Fourier transform. From above it is understood that we can use K_ℓ as a diagonal operator, however the image will have a pixel dimension of, for example 2048×2048 whereas the datacube will have dimensions of around 100×100 . The K_ℓ operator maps from the position in the image to the corresponding position in the datacube but when the matrices are different sizes the spatial frequencies will not correspond and miss-mapping will occur. It is obvious that an intermediate step is required to ensure that spatial mapping from the datacube to the image is accurate. This can be achieved by dividing the 2048×2048 image into 100×100 subimages for each projection p. These subimages will allow correct mapping and hence correct matching of frequencies as each subimage will have the same dimensionality as the corresponding plane of the datacube.

Further study of Hagen (2007) sheds some light on the Fourier domain implementation of this technique and explains the use techniques called forward and back projections. An understanding of the H matrix and the operation it performs would include taking a slice of the datacube and overlaying it on the focal plane array. A point spread function is then applied for the wavelength and projection. As the subimage pixel grid will not line up with the focal plane array, the subimage needs to be interpolated to allow matching points. This process needs to be repeated over all the projects and wavelengths. This approach is called the geometric projection approach and the understanding of this process allows other potential techniques to be used. The reverse projection technique that is performed by the EM and MART algorithms and can also be understood as locating the subimage on the focal plane array and calculating the wavelength which corresponds to that subimage. The subimage may now be applied but will not usually directly correspond so needs to be interpolated to find exact corresponding points. Although the subimage now corresponds to a plane of the datacube the plane will usually lie somewhere inbetween the wavelength required so a further interpolation is required along the wavelength axis. We can then add the subimage signal to the appropriate interpolated plane. The result is iterated and summed over all projections and wavelengths.

The spatial interpolation described above in the forward and back projections is easily handled in the Fourier domain using a complex exponential corresponding to the required shift. The point spread function blurring may also be achieved by multiplication with the optical transfer function.

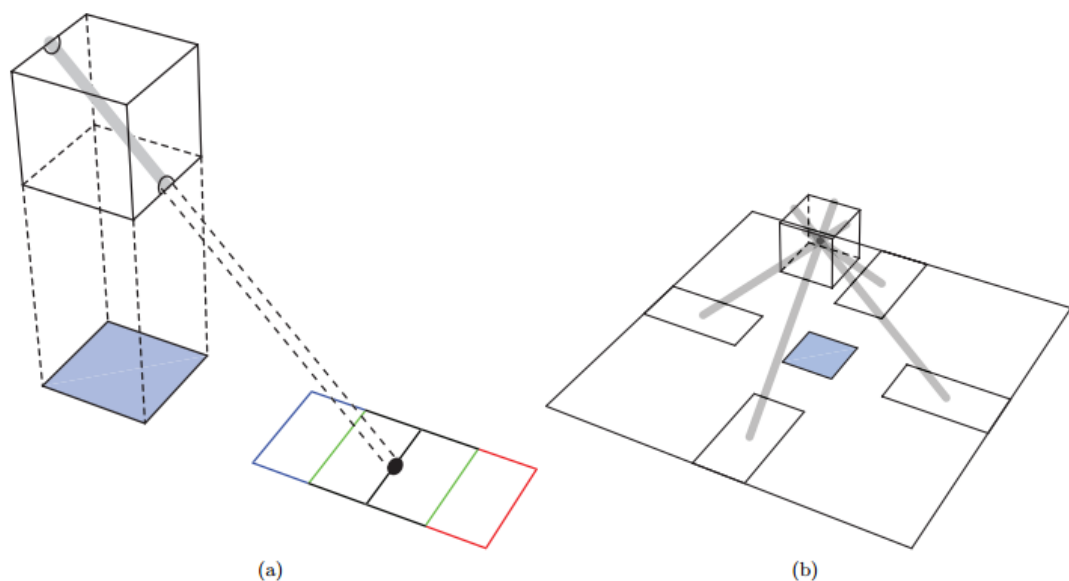


Figure 12: Representation of a single pixel being backprojected into the datacube in single projection in (a) and a set of four projections in (b) (Hagen, Dereniak & Sass 2007).

2.6. Relevant Australian Standards

2.6.1. Australian Standard AS3607 – 1989 Conductors-Bare overhead, aluminium and aluminium alloy-steel reinforced.

This standard outlines the material requirements and wire properties of aluminium, and aluminium alloy steel reinforced bare overhead conductors. There are a number of requirements in this standard which may have an influence on the spectral response of the different conductors and may help to explain the success or otherwise of the measurements.

AS3607 – 1989 requires the aluminium and aluminium alloys comply with alloy designations 1350, 1120, and 6201A which are defined in AS 2848.1. AS3607 – 1989 also has some requirements on the steel reinforcing which may affect spectral responses such as:

- The base metal for steel reinforcing wire shall be full-killed steel in accordance with AS 1442.
- The wire shall be either zinc-coated (galvanised-GZ), aluminium coated (aluminized-AZ) or aluminium clad (AC).
 - Zinc coated steel: The standard requires the zinc-coating use either the hot dip or electrolytic process, and shall pass a zinc coating test as per AS 1650. The standard also requires a coating not less than the following table:

TABLE 4.6
MASS OF ZINC COATING FOR STEEL WIRES

Nominal diameter of coated wire mm		Minimum coating mass g/m ²
≥ 1.55	≤ 1.80	200
> 1.80	≤ 2.24	215
> 2.24	≤ 2.72	230
> 2.72	≤ 3.15	240
> 3.15	≤ 3.55	250
> 3.55	≤ 4.25	260

Table 1. Mass of Zinc Coating for Steel Wires (Australian Standards 1989)

The standard also requires the purity of the zinc fed into the bath be not less than 98.5 percent if using the hot dip process. The wire before coating shall not be copper plated. The thickness and purity of the zinc coating required by this standard suggest that the spectral response of steel reinforcing and galvanised steel conductor will be that of almost pure zinc.

- Aluminium-coated steel: The standard requires that the aluminium used for aluminium coating shall be a maximum of 0.1% Copper and 0.5% Iron and be not less than the following table in mass:

**TABLE 4.8
MINIMUM MASS OF ALUMINIUM COATING
FOR STEEL WIRES***

Wire diameter mm	Minimum mass of aluminium coating g/m ²
1.60	77
2.25	80
2.50	86
3.00	92
3.50	98
3.75	104

* Wire with diameter intermediate to those shown shall have a coating mass equal to the next larger size.

Table 2. Minimum Mass of Aluminium Coating for Steel Wires (Australian Standards 1989)

The above requirements suggest that aluminium coated steel shall have a spectral response of very pure Aluminium.

2.6.2. Australian Standard AS 2848.1 – 1998 Aluminium and aluminium alloys – Compositions and designations – Wrought products.

Aluminium and aluminium alloys-compositions and designations goes into further detail regarding the aluminium and aluminium alloys used in overhead conductors. Alloy designations 1350, 1120, and 6201A are a product of the alloy designation system outlined in AS 2848.1. This system involves a 4 number designation with the first number indicating the major alloying element(s) which are as follows:

1XXX	Aluminium, 99.00% min
2XXX	Aluminium alloy - Copper
3XXX	Aluminium alloy – Manganese
4XXX	Aluminium alloy – Silicon
5XXX	Aluminium alloy – Magnesium

6XXX Aluminium alloy – Magnesium and silicon

7XXX Aluminium alloy – Zinc

8XXX Aluminium alloy – Other alloying element(s)

As the common conductor alloys in use in the Ergon Energy network are 1350, 1120, and 6201A, we will encounter:

1XXX Aluminium, 99.00% min

The second digit of the of this group of alloys indicates the special control of one or more individual impurities and if zero is unalloyed aluminium. The second and fourth digits refer to the digits to the right of the decimal place of the minimum aluminium percentage.

6XXX Aluminium alloy – Magnesium and silicon

The second digit in this group if zero indicates an original alloy, any other digits indicate alloy modifications. The second and fourth digits have no real significance except to identify the aluminium alloys in the group. A modification of an original alloy one or more of the following:

- The arithmetic mean of the modified limits less the arithmetic mean of the limits for the same alloying element in the original alloy must be below the values in the following table:

Arithmetic mean of an alloying element range of an original alloy %	Maximum allowable change to the arithmetic mean %
≤1.0	0.15
>1.0 ≤2.0	0.20
>2.0 ≤3.0	0.25
>3.0 ≤4.0	0.30
>4.0 ≤5.0	0.35
>5.0 ≤6.0	0.40
>6.0	0.50

Table 3. Alloying element limits (Australian Standards 1998)

- The addition or deletion of only one alloying element with limits having an arithmetic mean of not more than 0.30%

- The substitution of one alloying element for another to produce the same outcome.
- A change in limits for impurities
- A change in limits for grain refining elements
- Restricted iron or silicon limits which points to highly pure base metal.

2.6.3. Australian Standard AS 1746-1991 Conductors – Bare overhead – Hard-drawn copper.

This standard is the Australian Standard dealing with Conductors – Bare overhead – Hard-drawn copper and details the construction of the overhead HDDB conductors that will be encountered on the Ergon Energy network. AS 1746-1991 requires the copper used in bare overhead conductors comply with the high conductivity alloy, 110A standard as specified in AS 1279 and shall have a hard (H) condition as specified in AS 1574.

2.6.4. Australian Standard AS 1279-1985 Copper refinery shapes.

This standard outlines the copper refinery shapes required and states that the 110 standard is electrolytically refined tough pitch copper (Cu – ETP) as per table B1:

**TABLE B1
RELATED DESIGNATIONS**

Copper designation	Name	Other designations			Equivalent wrought designations		
		ISO	ASTM	BS	AS*	UNS	BS
Cu-CATH 1	Cathode copper— high purity	—	CATH Grade 1	Cu-CATH-1	—	—	—
Cu-CATH 2	Cathode copper	Cu-CATH	CATH Grade 2	Cu-CATH-2	—	—	—
Cu-ETP	Electrolytically refined tough pitch copper	Cu-ETP	ETP	Cu-ETP 2	110	C11000	C101
Cu-DLP	Phosphorus-deoxidized copper— low residual phosphorus	Cu-DLP	DLP	Cu-DLP	—	C12000	—
Cu-DHP	Phosphorus-deoxidized copper— high residual phosphorus	Cu-DHP	DHP	Cu-DHP	122	C12200	C106
Cu-Ag	Tough pitch copper-silver	Cu-Ag	STP	—	116	C11600	—

* Superseded Australian Standard designations.

Table 4. Related designations for copper refinery shapes (Australian Standards 1985)

AS1279 also defines Electrolytically refined tough pitch copper as copper that is produced by electrolytic deposition, which contains a controlled amount of oxygen in the form of copper(I) oxide. This form of copper is free of significant amounts of elements other than oxygen and suggests the spectral response of HDPC should be that of pure copper.

2.6.5. Australian Standard AS1574-1984 Copper and copper alloys – Wire for electrical purposes.

This standard referred to above is the standard for Copper and copper alloys – Wire for electrical purposes, and includes in its scope the following materials, tempers, and finishes:

Material	Temper	Finish
Oxygen-free electronic copper (C10100)	annealed hard	plain plain
Oxygen-free copper (C10200)	annealed hard	plain plain
Electrolytic tough pitch copper (C11000)	annealed hard	plain or tinned plain or tinned
Tin-bearing copper (149)	hard	plain

Table 5. Materials, tempers and finishes for copper and copper alloys (Australian Standards 1984)

As can be seen the standard has within its scope the form of copper used in overhead networks which is Electrolytic tough pitch copper (C11000) which may have a temper of annealed or hard and may have a plain or tinned finish. AS 1746-1991 above states that copper for use as HDPC should have a temper of hard which is outlined in clause 2.4.2 of AS1574 as having a minimum tensile strength of plain wire in the H temper, applicable to wire diameters 1 mm to 4.5 mm, in accordance with the following equation:

$$S = 480 - 20d \tag{2.18}$$

Where

S = minimum tensile strength, in megapascals

d = actual diameter of the wire, in millimetres.

And also requires that the minimum tensile strength of tinned wire in the H temper shall be 90% of the value calculated for untinned wire. AS1574 also requires that for wires with a

diameter less than 1.0 mm or greater than 4.50 mm the tensile strength shall be subject to agreement. Table 2.5 of AS1574 also outlines the electrical resistivity of plain wire:

TABLE 2.5
ELECTRICAL RESISTIVITY OF PLAIN WIRE

Alloy designation	Material	Temper	Resistivity at 20°C nΩ.m max.	Conductivity % IACS min.
C10100	Oxygen-free electronic copper	O	17.241	100
		H	17.77	97
C10200	Oxygen-free copper	O	17.241	100
		H	17.77	97
C11000	Electrolytic tough pitch copper	O	17.241	100
		H	17.77	97
149	Tin-bearing copper	H	23.60	73

Table 6. Electrical resistivity of plain wire (Australian Standards 1984)

This table shows that the material used for HDBC which is typically C11000 electrolytic tough pitch copper in a hard temper has a resistivity at 20°C is 17.77 nΩ. m max. and has a minimum conductivity of 97% IACS. It is not anticipated that these requirements will have a significant or measureable impact upon the spectral reflectivity of the materials.

2.7. Chapter Summary

The literature review performed in this chapter presented previous studies carried out by various authors and provided a means to achieve the project objectives. Information was presented on what the terms reflectance, emittance and absorbance mean, the factors that affect spectral measurements, a way to measure the repeatability of the measurements, and achieved the objective of the project in investigating the relevant Australian standards which provide information on the metallurgy of bare overhead conductors.

3. Methodology

3.1. Chapter Overview

The methodology chapter outlines the way in which the project objectives were achieved. This chapter will bring context to the remaining dissertation chapters explaining how they relate to the project objectives. The overarching steps required to achieve the project objects are:

- Research
- Measurements using a commercial spectrometer
- Confirmation of theory using image spectroscopy
- Analysis of the results using the correlation co-efficient to measure the constancy of the spectral results under various conditions using a number of conductor samples

Further information on each of these steps is included in the following chapters.

3.2. Research

The research into the various factors that will contribute to the successful achievement of the objectives is outlined in chapter 2 the literature review. The mechanics of how photons of light are reflected and refracted from the particles that make up a material was explained which is useful in understanding our results. Similarly the factors that affect spectral measurements including atmospheric and instrument design will also allow a more thorough understanding of the results achieved. A suitable measure for the repeatability of the measurements will allow a greater understanding of the suitability of spectral analysis in identifying bare overhead conductors. Finally the various Australian standards allow a greater understanding of the materials that make up the various conductors and therefore the expected results of the spectral reflectance measurements.

3.3. Measurements using a commercial spectrometer

The principles of operation of many newer generation plug and play usb powered spectrometers are essentially the same as was found in the literature review chapter. Again the light enters through a slit (in this case $50 \times 1000\mu\text{m}$) and the divergent light collimated using a curved mirror. The incoming light is then split into the various wavelengths of light using a diffraction grating which is then focused onto the CCD of the device using a convex mirror. The primary difference between the version using a consumer camera and the

commercial version is that the commercial version uses angled mirrors to create a much shorter total physical length and therefore is much more convenient in operation.

In this case testing was carried out using an Ocean Optics USB4000 plug and play miniature fibre optic spectrometer with a diffuse sensor (Ocean Optics, Inc., USA). This particular spectrometer has been employed at the USQ to measure spectral irradiance on plant leaves. The Ocean Optics USB4000 has a bandwidth of 200 nm to 850 nm and uses a 600 line blazed grating, a blaze wavelength of 400 nm and a slit width of 25 μm . This translates to an average integration step of 0.2nm. The spectrometer was set up in a laboratory at the USQ engineering department and a number of measurements were taken of various conductor samples. When using a portable spectrometer, any reflected light within the field of view of the fibre patch cord will contribute to the reflectance curve measured therefore if the subject is too far away from the fibre then the result will be polluted by unintended reflected light.

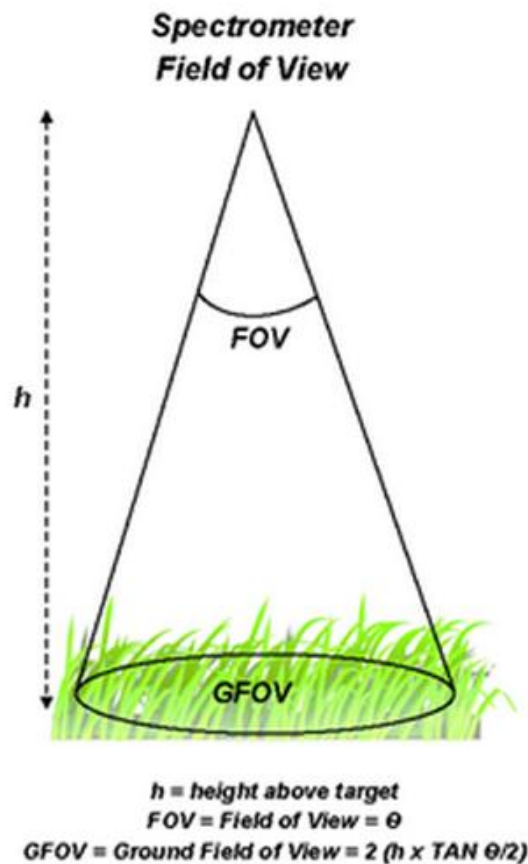


Figure 13: Spectrometer field of view calculations (<http://discover.asdi.com/bid/97740/Expert-Tip-Understand-Your-Field-of-View-When-Taking-Reference-Measurements>)

The fibre patch cord used in this example has a field of view of 25°, and taking into account the smallest conductor measured has a diameter of 5.7mm we can calculate the height required as:

$$GFOV = \text{Ground Field of View} = 2(h \times \tan \frac{\theta}{2}) \quad (3.1)$$

As GFOV = 5.7mm max

$$5.7 = 2(h \times \tan \frac{25}{2})$$

$$\frac{5.7}{2} = h \times \tan \frac{25}{2}$$

$$\frac{2.85}{0.222} = h$$

$$h = 12.84 \text{ mm}$$

Therefore the maximum height the end of our fibre can be from the sample is 12.84 mm.



Figure 14: Actual setup for spectral measurements using an Ocean Optics USB 4000.

A number of measurements were taken of the following conductors:

- 19/2.00 Copper
- 7/2.75 Copper
- 7/2.00 Copper
- 7/1.75 Copper
- 3/12 Galvanised Steel
- 7/2.75 Galvanised Steel
- 19/2.00 Galvanised Steel
- 19/2.75 Galvanised Steel

- 3/4/2.5 Aluminium Conductor Steel Re-enforced
- All Aluminium Alloy Conductors Flourine
- All Aluminium Alloy Conductors Helium
- All Aluminium Alloy Conductors Iodine
- All Aluminium Alloy Conductors Libra
- All Aluminium Conductors Mars
- All Aluminium Conductors Moon

The board of conductors tested is in the below figure. The top conductors are aluminium, the second row is aluminium alloy, the third row contains copper, and the fourth row contains galvanised steel conductors. The bottom two rows contain samples of insulated low voltage conductor which were not tested.



Figure 15: The range of conductors tested

These measurements were taken of each conductor under a halogen spotlight (11200 lux), fluorescent lighting (1720 lux), and low levels of daylight (125 lux) to provide measurements under a wide variety of lighting conditions. The integration time of a spectrometer refers to how long the detector is allowed to collect photons of light before the accumulated charge is sent to the converter for processing. Long integration times are a sign of excessively low lighting levels and lead to the introduction of noise in the measurement. Light levels were adjusted to ensure integration times were kept under one second.

3.4. Confirmation of theory using image spectroscopy

The consumer camera chosen for this part of the project was a Nikon D700 due to the author's ready access to this particular model and it fulfils the requirements of having a high sensitivity CCD sensor and the ability to capture high dynamic range (HDR) photography. HDR is a photographic method which takes many exposures of the same scene and blends them together to provide a well exposed image of scenes with a wide variance in lighting. In this case the requirement for HDR ability was particularly important to obtain enough light at the weaker frequencies to produce a useful reflectance curve by extending the dynamic range of the image.

The optical components chosen were primarily driven by a need for ready availability and the ability to create the optical path needed to the camera CCD without any modification rendering the component useless for post dissertation use. As modern lenses are of a high standard of imaging accuracy and to a large extent prevent the introduction of artefacts, it was found that the author already possessed most of the required lenses to provide a suitable optical path. The initial lens combination consisted of:

- A Nikon 50mm Nikkor F 1:1.8 lens as the re-imaging lens.
- A 28-75mm Tamron Aspherical LD XR Di SP F2.8 lens as the imaging lenses
- A manual Nikkor F 1:4.5 35-105mm lens as the collimating lens.

This combination of lenses was put together with lengths of PVC tubing purchased at Masters hardware store and combined with a sheet of diffraction gel due to inexpensive examples being commonly available that are holographically produced, are very accurate, readily available, and relatively inexpensive. In this case a sheet of Edmund optics, stock no. nt54-509 was purchased. This combination of lenses provided an optical path that was able to meet the requirements of:

- The first diffraction modes must fall entirely within the CCD sensor
- The first modes must also be far enough away from the zero mode

- The colour channels must not overlap

However due to the relatively large F stop of the Nikkor 35-105mm lens at F4.5 it was discovered that there was not enough light making it through the optical path to the camera CCD. Another collimating lens was purchased online being an achromatic macro lens which was 100mm focal length due to it being much lighter in weight and having a much more suitable ability to pass light.



Figure 16: The original Nikkor 35-105mm lens on left and 100mm achromatic lens on right

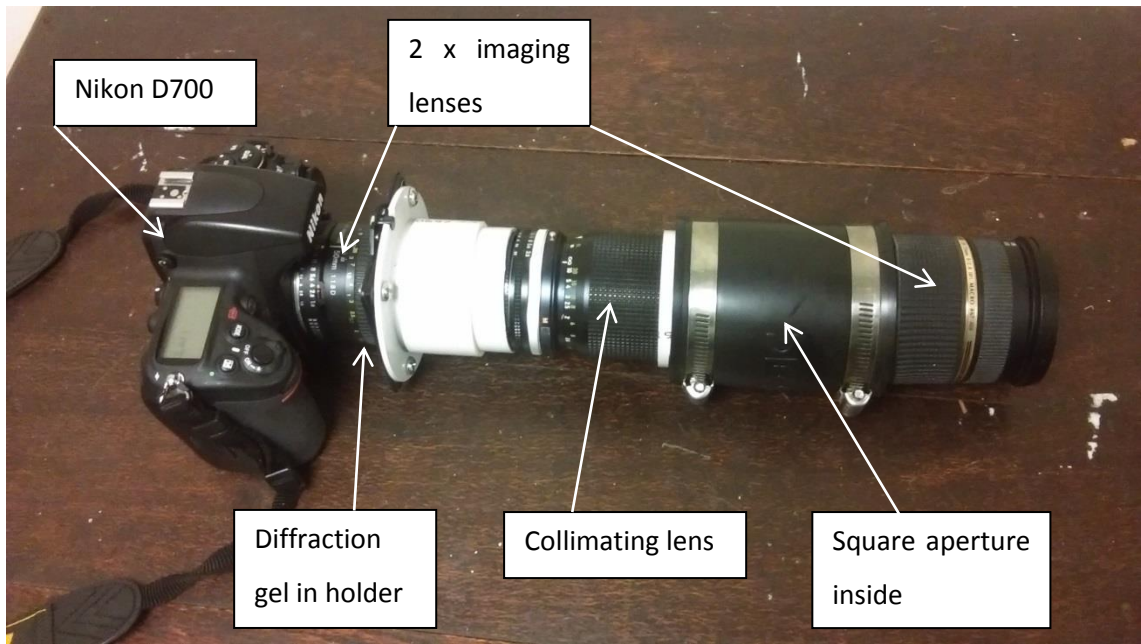


Figure 17: The assembled consumer camera

The only somewhat problematic element is the particular and precise arrangement of the optical elements in a consumer camera to successfully create an optical path that divides the spectral data by directing the different spectrums onto the Bayer filter array sensor at the angles required to produce a CTIS image. The delicate nature of the very long combination of lenses connected by somewhat imprecise plumbing fittings and a requirement to direct the sampled light through a 2 mm slit aperture continued to be problematic throughout the measurements, and made measurements anywhere other than strictly controlled laboratory conditions with multiple stands and props all but impossible. The all-aluminium conductor proved to be the only sample that reflected enough light to obtain a useable measurement.

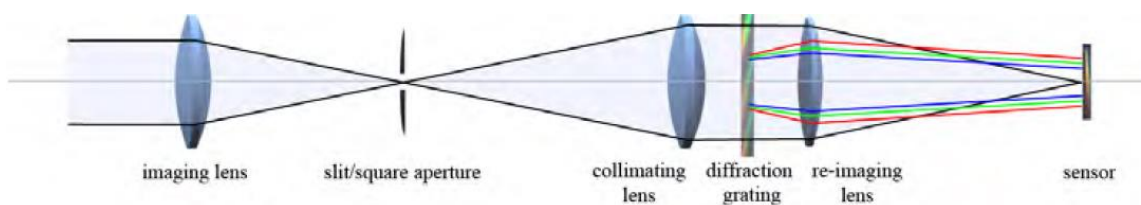


Figure 18: A representation of the optical path required to successful measurements.

The use of a slit aperture was considered as this may have provided a high resolution image, however this idea was discarded in favour of the square aperture as the slit aperture would only record a column of the measured scene whereas the square aperture created a configuration much more suited to computed tomography imaging. The imaging lens was used at the minimum focal length of 28 mm to attempt to maximise the light intensity and alleviate some of the problems with intensity discussed above. This focal length has the effect of concentrating the image onto a much smaller area of the camera sensor and maximising the

light detected per pixel. As only a small area at the centre of the sensor is used this method also reduces the chance of distortion. The measurements taken indicate that a smaller focal length would have been desirable.

The advantage of the square aperture over the slit aperture is that while it is possible to extract each single response with a slit aperture, these responses are superimposed when using a square aperture. The projection of these superimposed responses is represented by matrix H which operates on the vector \vec{f} which contains the serialized voxels of the data cube. The action of the diffraction gel produces a further vector \vec{g} which then represents the serialized version of the image pixels the CTIS system measures. This process is represented by the formula:

$$\vec{g} = H\vec{f} \quad (3.2)$$

Where H is an M x N matrix, M is the number of pixels in the image and N being the number of voxels in the data cube. Each column contains five entries at each position at one wavelength and the zero mode. This creates a H matrix which is very large but also sparse. This process produces a non-square matrix requiring an iterative process to solve for \vec{f} .

This iterative process could be achieved a number of different ways, however for simplicity an expectation maximisation algorithm was chosen due to previous authors work in this area (Shepp & Vardi 1982). Shepp found this method to be relatively simple to implement, produce consistent results and converges relatively quickly. Although it is possible, for the purpose of this project no noise reduction was carried out.

The expectation maximisation algorithm was first used to provide an initial guess (Shepp & Vardi 1982):

$$f_n^{k+1} = \frac{f_n^k}{\sum_{m=1}^M H_{mn}} \sum_{m=1}^M H_{nm}^T \frac{g_m}{(Hf^k)_m} \quad (3.3)$$

Using the above formula we now have a fully defined H matrix and can solve the data cube of the measured CTIS image. Each colour is separated and a H matrix is created for each of the four colour channels. As the camera used employed a CCD Bayer array in the RRGB format two green channels were created and to avoid unnecessary processing the wavelength is only solved when its resultant response function is not zero. The resultant four H matrices for each colour were 161,604 x 215,818 for red, 161,604 x 223,260 for each of the green channels and 161,604 x 186,050 for the blue channel. Approximately 15 – 30 iterations were required to successfully converge however this proved to be one of the more problematic parts of the image spectrometer implementation with many non-convergences experienced. Although the

square aperture, and the built in low pass filter of the camera reduce aliasing artefacts were still evident in almost all of the measurements. As the spectra are super imposed upon one another if an artefact is present it is present through the whole of the reconstructed result. An unintentional solution was found when the scene was shot out of focus. This method appeared to reduce the artefacts but did also reduce the resolution of the measurement.

The use of Matlab and a regular computer to resolve the data cube into a unique spectral curve is the last element that will allow a cost effective method of image spectroscopy for the purpose of this project. The final implementation of such a method for real time use would likely not involve these methods as there are some disadvantages in exposure time and post processing time and effort in Matlab, but the concept can be tested within the budget allocated to this project in this way.

A simple Matlab code has been developed which uses Fourier transforms and multi-threading to resolve the HDR data cube:

```
function [f_out] = expectmax(H,g,iter)
f_iter = (H')*g; %initial guess
h_sum = sum(H,1); %precompute fixed sums
for m=1:iter
g_iter = H*f_iter;
g_div = g./g_iter;
g_div(isnan(g_div) | isinf(g_div)) = 0;
% open matlabpool for multithreading
parfor n=1:length(f_iter)
f_next(n)=(f_iter(n)'./h_sum(n))'.*sum(H(:,n).*g_div);
end
f_iter = f_next';
end
f_out = f_iter;
end
```

In practice this code resolves a test data set in approximately in 11 minutes on a 16 core (4 processors) AMD Opteron 2 GHz system.

4. Results and Discussion

4.1. Chapter Overview

All measurements were completed successfully with most curves appearing in the appendix section of this dissertation. There were two methods of spectroscopy used to measure conductor samples, a commercial plug and play spectrometer and an experimental combination of lenses and a consumer camera to test the theory of image spectroscopy. Measurements of the aluminium conductors, the aluminium alloy conductors, and the galvanised steel conductors using the Ocean Optics USB4000 gave results with a high degree of correlation (consistency) regardless of the sample size or sample age or lighting. Copper however gave consistent results between samples of similar surface patina, but results had a low correlation when surface conditions varied greatly. The constructed image spectrometer proved problematic, however did give two results which correlated highly with each other but gave only moderate correlation with the results obtained using the commercial image spectrometer.

4.2. Commercial USB plug and play spectrometer results

Each of these samples was measured at three differing light levels being under a halogen spotlight (11200 lux), fluorescent lighting (1720 lux), and low levels of daylight (125 lux). The resultant curves are produced in the appendix and were analysed using the correlation formula to produce a correlation co-efficient to indicate the consistency of the results.

4.2.1. Galvanised Steel under spotlight

The commercial plug and play spectrometer gave very consistent results regardless of the size of the sample measured. The galvanised steel conductors measured were:

- 3/12 Galvanised Steel
- 7/2.75 Galvanised Steel
- 19/2.00 Galvanised Steel
- 19/2.75 Galvanised Steel

The galvanised steel reflectance curves as measured under a halogen spotlight are shown in appendix D and the correlation co-efficients for these results are as follows:

	7/2.75 SC/GZ	19/2.00 SC/GZ	19/2.75 SC/GZ
3/12 SC/GZ	0.999598078	0.99830144	0.998791427
7/2.75 SC/GZ	NA	0.997557058	0.998282258
19/2.00 SC/GZ	0.99830144	NA	0.999470111
19/2.75 SC/GZ	0.998282258	0.999470111	NA

Table 7. Correlation co-efficients for galvanised steel reflectance curves under spotlight

These results show a very high correlation co-efficient and therefore exhibit very consistent results.



Figure 19: A close up photograph showing the typical surface characteristics of the actual galvanised steel conductors tested.

4.2.1. Galvanised steel conductors under fluorescent and low level daylight

The galvanised steel reflectance curve as measured under fluorescent lighting are shown in appendix E against the same size under a halogen spotlight and the correlation co-efficients for these results are as follows:

	19/2.00 SC/GZ Fluorescent	19/2.00 SC/GZ Daylight	19/2.00 SC/GZ Spot
19/2.00 SC/GZ Spot	0.983807283	0.980233309	NA
19/2.00 SC/GZ Daylight	0.964110473	NA	0.980233309
19/2.00 SC/GZ Fluorescent	NA	0.964110473	0.983807283

Table 8. Correlation co-efficients for galvanised steel reflectance curves under fluorescent and low level daylight

These results show a very high correlation co-efficient and therefore exhibit very consistent results despite the inherent noise introduced by the lower light levels of the fluorescent and low daylight lighting methods.

4.2.1. Copper conductors under spotlight

The commercial plug and play spectrometer gave very inconsistent results for differing surface conditions and lighting conditions of the copper. The copper conductors measured were:

- 7/1.75 Copper
- 7/2.00 Copper
- 7/2.75 Copper
- 19/2.00 Copper

The copper reflectance curves as measured under a halogen spotlight are shown in appendix F and the correlation co-efficients for these results are as follows:

	7/1.75 Cu	7/2.75 Cu	19/2.00 Cu
7/2.00 Cu	0.995269	0.934627	0.41398341
7/1.75 Cu	NA	0.944453	0.35660958
7/2.75 Cu	0.934627	NA	0.49251366
19/2.00 Cu	0.35661	0.492514	NA

Table 9. Correlation co-efficients for copper reflectance curves under spotlight

These results show a very high correlation co-efficient between 7/2.00, 7/1.75, 7/2.75, however show a relatively low correlation between the 19/2.00 sample and the other conductors. As the spectrum analysed is in the visible region, this confirms the subjective visual impressions that the 19/2.00 sample looked very different from the other samples and was significantly tarnished due to much more time in the elements.

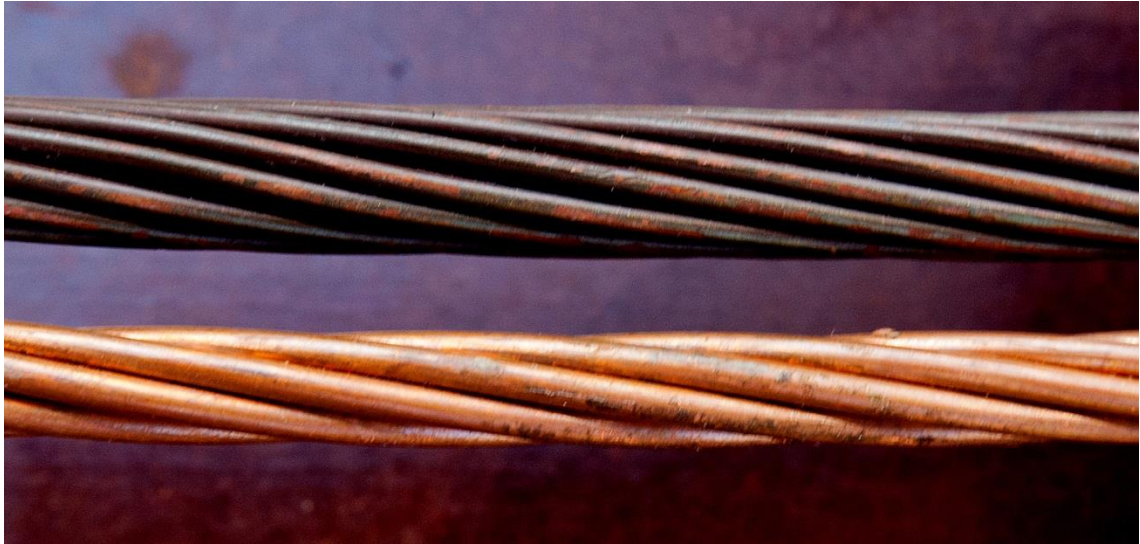


Figure 20: A close up photograph showing the different surface characteristics of the actual copper conductors tested.

4.2.1. Copper conductors under fluorescent and low level daylight

The copper reflectance curves as measured under the differing light conditions are shown in appendix F and the correlation co-efficients for these results are as follows:

	7/2.75 daylight	7/2.75 fluorescent	7/2.75 Cu spot
7/2.75 Cu spot	0.422105659	0.559380753	NA
7/2.75 daylight	NA	0.844153061	0.422105659
7/2.75 fluorescent	0.844153061	NA	0.559380753

Table 10. Correlation co-efficients for copper reflectance curves under fluorescent and low level daylight

These results show a relatively low correlation co-efficient between the 7/2.75 copper samples taken under the three differing lighting types and levels. The only exception was the fluorescent and low level daylight samples which still showed a greater than 0.8 correlation.

The conclusion from these results is that the reflectance curves of the copper samples are affected significantly by variations in lighting and surface weathering in the visible spectrum of light.

4.2.1. All aluminium conductors under spotlight

The commercial plug and play spectrometer gave very consistent results for differing surface conditions and lighting conditions of the all-aluminium conductors. The all-aluminium conductors measured were:

- Libra
- Moon
- Mars

The all-aluminium reflectance curves as measured under a halogen spotlight are shown in appendix G and the correlation co-efficients for these results are as follows:

	Mars	Moon
Libra	0.998238	0.998068
Mars	NA	0.999855

Table 11. Correlation co-efficients for all aluminium reflectance curves under spotlight

These results show a very high correlation co-efficient between Libra, Mars and Moon. As the spectrum analysed is in the visible region, this confirms the subjective visual impressions that all samples appear very similar to the human eye.



Figure 21: A close up photograph showing the typical surface characteristics of the actual aluminium and aluminium alloy conductors tested.

4.2.2. All aluminium conductors under fluorescent and low level daylight

The all-aluminium reflectance curves as measured under the differing light conditions are shown in appendix H and the correlation co-efficients for these results are as follows:

	Mars Daylight	Mars Fluorescent
Mars Spot	0.783032483	0.752574072
Mars Daylight	NA	0.945930315

Table 12. Correlation co-efficients for all aluminium reflectance curves under fluorescent and low level daylight

These results show a very moderate correlation co-efficient between Libra, Mars and Moon under the differing lighting conditions. Interestingly the two lower lighting levels correlate a lot more with each other than with the flood lit measurement.

4.2.3. Comparison of all aluminium conductors and all aluminium alloy conductors under spotlight

One of the primary aims of the specification of this project was to test the ability of spectral measurements to differentiate between all aluminium and all aluminium alloy conductors. With that aim measurements were carried out under spot light conditions with the results appearing in appendix I. The commercial plug and play spectrometer gave very consistent results for the two different conductors with a very high correlation co-efficient of **0.998421**. It would appear that the Ocean Optics USB 4000 device is incapable of differentiating between these two conductor types in the visible spectrum.

4.3. Consumer camera image spectroscopy results

4.3.1. Establishing the calibration of the results of the image spectroscopy implementation

There are various methods for establishing the accuracy of the spectral curve. Firstly the consumer camera will be calibrated using a known light source. A fluorescent lamp will provide the necessary lighting over the whole of the aperture and has a well-known and understood spectrum. The fluorescent spectrum has three distinctive and consistent peaks at red

(611.3nm), blue (435.7nm) and green (546.1nm). Figure 13 shows the expected CFL spectral curve as obtained from the Aster Spectral Library.

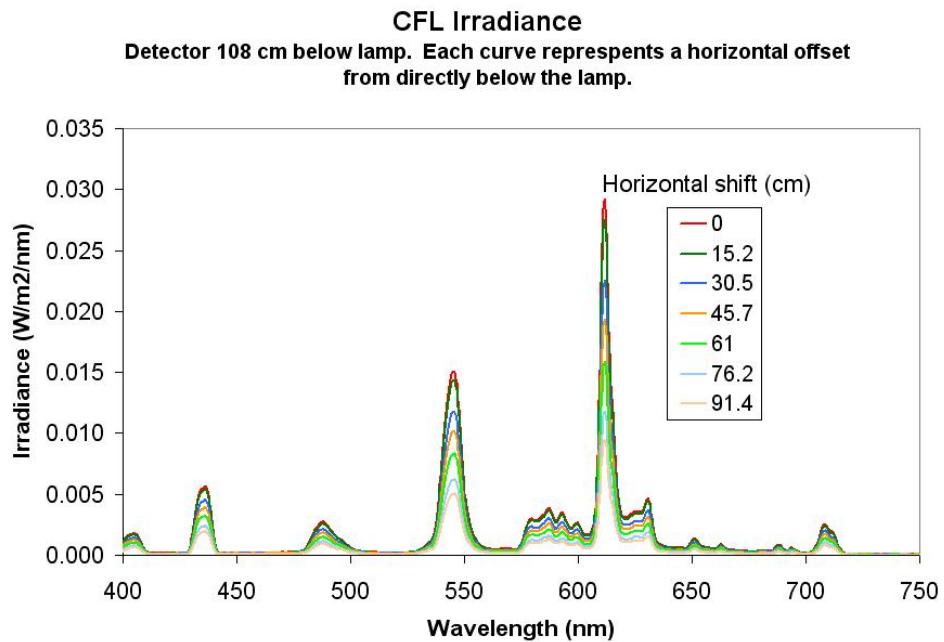


Figure 22: Fluorescent Spectrum Source: Aster Spectral Library Baldrige, A. M., S.J. Hook, C.I. Grove and G. pp. 711-715

Figure 14 shows the obtained results using the image spectroscopy implementation. A relatively noise free curve was obtained as the light source was shone directly into the lens of the first imaging lens and provided a very high level of light photons. The obtained measurement of the fluorescent spectrum also has three distinctive and consistent peaks at red (610nm), blue (435nm) and green (545nm) proving the calibration of the device is at an acceptable level for the purposes of these measurements.

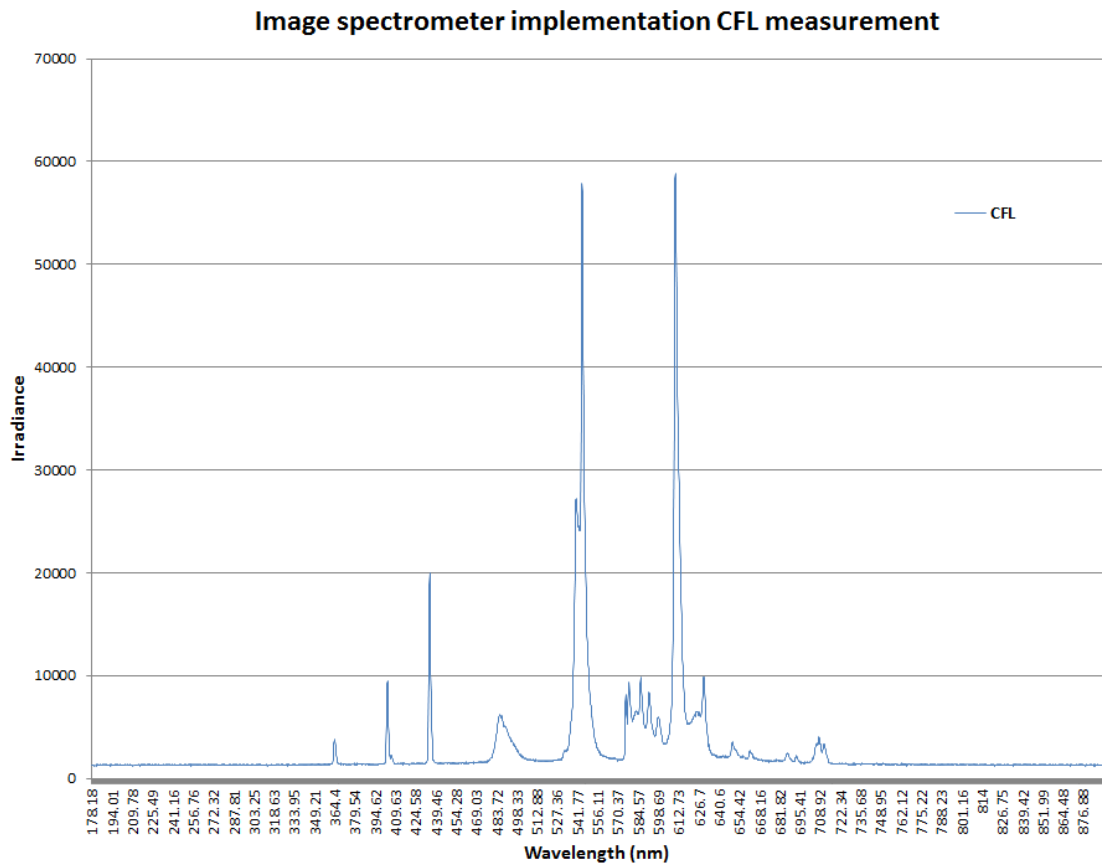


Figure 23: Fluorescent Spectrum Measurement using an image spectrometer created from a consumer camera.

After the modified consumer camera was proven to be calibrated, repeated tests were then attempted on numerous known conductors in various lighting situations both overhead and in a test environment.

4.3.1. Measurements using the image spectroscopy implementation

As previously discussed measurements using the consumer camera version of the image spectrometer proved to be extremely problematic with only two successful measurements using a very high level of subject lighting. The typical measurement is as per the following figure:

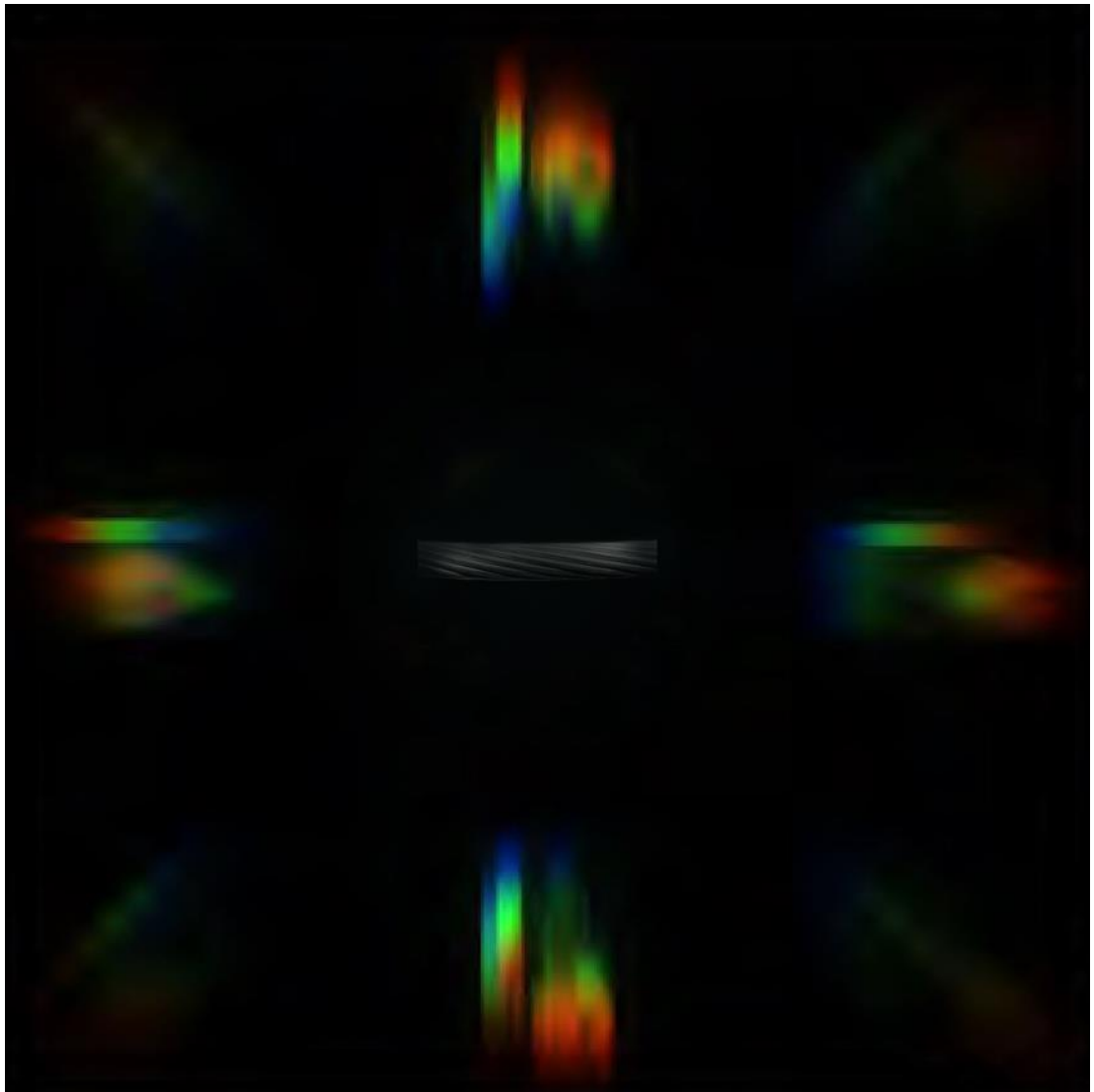


Figure 24: Spectral Measurement using an image spectrometer created from a consumer camera. The data cube was constructed from this measurement.

As can be seen from the above figure the diffraction gel slits the light into its component colours and the combination of imaging, re-imaging, and collimating lenses focuses the diffracted light onto the CCD of the Nikon D700. This result was resolved using Matlab to produce a spectral curve. Only the calibration using a compact fluorescent and two other measurements, one of an aluminium conductor, and one of an aluminium alloy conductor were able to be carried out.

The all-aluminium and aluminium alloy reflectance curves as measured with the D700 image spectrometer are shown in appendix I and a comparison of the correlation co-efficients for these results and those measured with the Ocean Optics USB4000 are as follows:

	AAC D700	AAAC D700	AAAC OO
AAAC D700	0.99935	NA	NA
AAC OO	0.771382	0.78279828	0.998235
AAAC OO	0.780294	0.791456395	NA

Table 13. Correlation co-efficients for all aluminium and aluminium alloy reflectance curves using both measuring instruments (OO denotes those measured with the USB4000)

These results show a very a strong correlation co-efficient between the all-aluminium and aluminium alloy conductors as measured by the D700 image spectrometer. There is only however a moderate correlation between results captured by the D700 image spectrometer and those captured by the Ocean Optics USB4000 commercial spectrometer.

5. Conclusions & Recommendations

5.1. Chapter Overview

This chapter concludes that the project objectives were met with a high degree of success with only the problematic measurements using the constructed image spectrometer giving somewhat incomplete results. The technology is certainly worthy of further investigation and negotiations are underway to investigate the incorporation of image spectroscopy into a commercial service provider.

5.2. Achievement of the Project Objectives

There were five objectives in the project specification with another two objectives as time permits. The first of these objectives:

- ❖ Research conductor metallurgy to identify the composite metals that make up commonly used overhead conductors.

This objective was completed in chapter two in the literature review. Various Australian standards were reviewed to understand the requirements in producing conductors including how the metals are forged and to what hardness, what alloying components are required and the method of galvanisation of conductors. Furthermore an analysis of conductor failures was carried out in chapter one to better understand the rates of failure of each of these conductor types.

The second objective:

- ❖ Critically evaluate current conductor identification techniques.

This objective was completed in chapter one also with research carried out on current identification practises. The evaluation resulted in the conclusion that conductor identification within the Ergon Energy network is carried out almost exclusively by eye with a scratch test carried out only if an alloyed conductor is suspected. The relatively primitive current methods confirm the value of the research carried out in this project and that spectral analysis of overhead conductors is indeed the application of an existing technology in a way not previously investigated.

The third objective:

- ❖ Evaluate spectroscopy as a method of identifying overhead conductor materials under laboratory conditions.

This objective is the primary objective of the project and was carried out using a USB plug and play spectrometer with varying degrees of consistency across the range of conductor types. As the measurements were primarily taken in the visible spectrum, metals that have a changing surface appearance due to weathering, pollution or other factors showed a lack of consistency in their spectral measurements.

Galvanised steel conductor showed a high consistency in measurements obtained over the visible spectrum regardless of weathering of the sample, size of the sample, or lighting conditions tested with an average correlation co-efficient of **0.989624** which equates to a **very strong correlation**.

All Aluminium conductor also showed a high consistency in measurements obtained over the visible spectrum regardless of weathering of the sample, size of the sample, however some reduced correlation was measured in poor lighting conditions. Despite this loss in correlation in low light conditions, all samples and lighting conditions tested resulted in an average correlation co-efficient of **0.91295** which equates to a **very strong correlation**.

Copper conductor showed a fair consistency in measurements obtained over the visible spectrum. Results were consistent regardless of the size of the sample, however lighting conditions and surface conditions had a large effect on results with all samples and lighting conditions tested having an average correlation co-efficient of **0.657912** which equates to a **fair correlation**.

An attempt to differentiate between all aluminium and all aluminium alloy conductor found that the Ocean Optics USB4000 when measuring in the visible spectrum was unable to differentiate between the two conductors. Measurements of the two conductors had a **very strong correlation** of **0.998421**.

The fourth objective:

- ❖ Attempt the construction of an image spectrometer using a consumer camera to further understanding and test the device on a conductor sample.

This objective was somewhat ambitious and was completed with a limited degree of success. Only three measurements were able to be successfully carried out using the constructed image spectrometer being a compact fluorescent calibration measurement and two measurements of aluminium conductor. The difficulties in producing accurate, useable and consistent results were primarily caused by the very long and fragile nature of the combination of lenses and filters used. As an alignment in the sub millimetre were required to allow the light photons to navigate the optical path any slight misalignment resulted in no usable measurement being

recorded. The light photon levels required to light the subject was also comparatively very high to ensure enough light made it through the combination of three lenses, a square slit filter, and a diffraction grating, and then fall onto the camera sensor and produce a useable measurement.

The fifth objective

- ❖ Submit an academic dissertation on the research.

This objective has been completed with the submission of this dissertation.

There were also two objectives listed as time permits, the first of these being:

- ❖ Evaluate methods of remote conductor diameter measurement to use in conjunction with hyper spectral analysis to definitively identify overhead conductor.

Not a lot of time has been devoted to the completion of this objective, although contact was made with a representative of C. R. Kennedy survey solutions who recommended the Leica Nova MS50 as an example of the current range of surveying devices which may be suitable for the task of remotely measuring conductor diameters. This particular device may not be the ideal device for this particular application, but does possess the capability required. The Leica Nova MS50 is capable of measuring 1000 points per second up to 300 metres with millimetre scan precision and has a scan range of up to 1000 metres. An example of the measurements the Leica Nova MS50 is capable of is in the following figure.

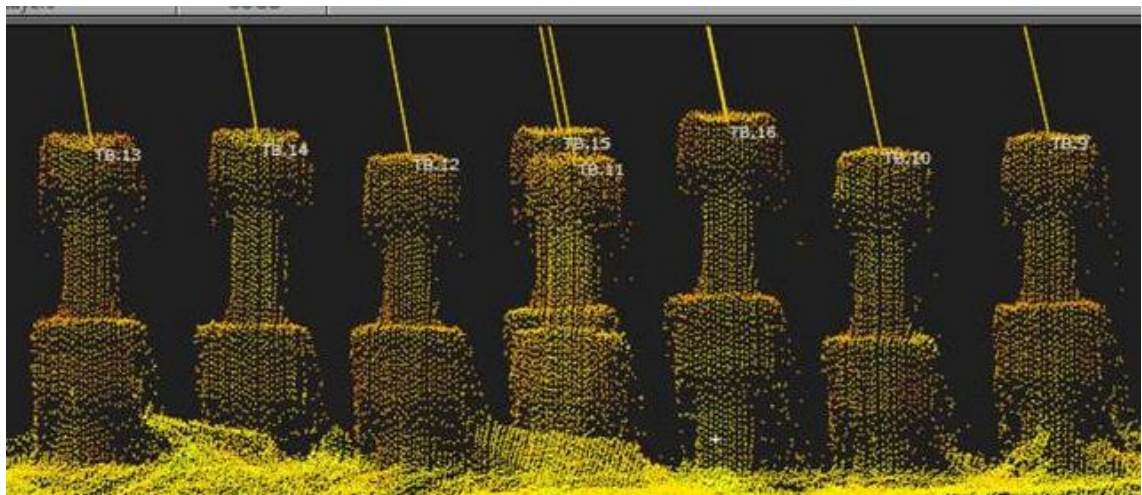


Figure 25: Measurement of some 140 mm x 20 mm bolts at 300 metres using the Leica Nova MS50 (courtesy of C. R. Kennedy Survey).

The second objective as time permits was:

- ❖ Investigate the feasibility of integrating conductor material identification and diameter measurement into the ROAMES LiDAR aircraft which overflies the entire Ergon Energy network each year.

This objective has progressed to the point where talks have taken place with Fugro ROAMES with very positive feedback received. This objective has been placed in a program of initiatives to investigate further. Current commitments have limited the amount of time and effort that can be devoted to the initiative at present however it is hoped that spectral imaging will be seriously investigated with a view to incorporating the technology into the ROAMES workflow in the future.

5.3. Feasibility

This project has shown that as the current identification methods involve identification by eye only, spectral imaging has the potential to save vast amounts of money if conductor identification were to be carried out over the approximately one millions spans of conductor in the Ergon Energy network. As such the technology will be investigated further.

5.4. Recommendations / Further Work

It is recommended that further investigation be carried out involving spectral measurements. These investigations should include but not be limited to:

- ❖ Investigate if measurements of copper conductors can result in more consistent results if measured further in the ultra violet and infra-red parts of the spectrum. As measurements in this project were carried out in the visible part of the spectrum, it is a somewhat predictable outcome that if the copper patina results in a visually different surface then the measurement of the surface using the visible part of the spectrum would also differ.
- ❖ Investigate if the use of an image spectrometer in an aircraft would result in reliable conductor identification particularly in an urban area with the clutter of metallic objects that would likely be present. With the current military and scientific uses that spectral measurement is being put to it is suspected that the capability exists, however this would need to be proven before moving to any type of commercial commitment.
- ❖ Investigate if the spectral measurement could be combined with a conductor diameter measurement and a positional measurement. This would help to ascertain if in an urban environment with both high voltage distribution conductor and low voltage conductor of a different metal on the same poles, the correct conductor diameter and metallurgy could be attributed to the correct conductor spatially. The current Fugro

ROAMES sensors have the measurement of the positional attributes available to a high degree of accuracy, but if this data can be attributed to the spectral measurement requires some investigation.

References

Bibliography

Australian Energy Regulator 2015, *PRELIMINARY DECISION Ergon Energy determination 2015-16 to 2019-20*, viewed 23 June 2015, <https://www.aer.gov.au/sites/default/files/AER%20-%20Preliminary%20decision%20Ergon%20Energy%20-%20Overview%20-%20April%202015_0.pdf>.

Australian Standards 1984, *AS1574 Copper and copper alloys - Wire for electrical puposes*, viewed 14 June 2015.

Australian Standards 1985, *AS1279 Copper refinery shapes*, viewed 14 June 2015, <>.

Australian Standards 1989, *AS3607 Conductors-Bare overhead aluminium and aluminium alloy-steel reinforced*, viewed 16 June 2015, <>.

Australian Standards 1991, *AS1746 Conductors - Bare overhead - Hard - drawn copper*, viewed 14 June 2015, <>.

Australian Standards 1998, *AS2848.1 Aluminium and aluminium alloys - Compositions and designations -Wrought products*, viewed 25 January 2015, <>.

Baldrige A M, HJGIRG 2009, 'The ASTER Spectral Library Version 2.0', *Remote Sensing of Environment*, 2009, pp. 711-715.

Chi, C, Yoo, H & Ben-Ezra, M 2010, 'Mulit-spectral imaging by optimized wide band illumination', *Computer Vision*, January 2010, pp. 140-151.

Clark, RN 1999, 'Spectroscopy of Rocks and Minerals, and Principles of Spectroscopy', in AN Rencz (ed.), *Manual of Remote Sensing*, John Wiley and Sons, Inc, New York.

Curtiss, B & Goetz, AFH 2001, *Field Spectrometry techniques and isnrumentation: Analytical Spectral Devices Inc*, viewed 23 March 2015, <<http://www.asdi.com/Field%20Spectroscopy>>.

Debevec, PE & Malik, J 1997, *Recovering high dynamic range radiance maps from photographs*, ACM Press/Addison-Wesley Publishing Co.

Descour, MR, Derenia, EL & Dubey, AC 1995, 'Mine detection using instantaneous spectral imaging', *Detection Technologies for Mines and Minelike Targets*, pp. 286-304.

Duggin, MJ & Philipson, WR 1982, 'Field measurement of reflectance: some major considerations', *Applied Optics*, 1982, pp. 2833-2840.

Du, H, Tong, X, Cao, X & Lin, S 2009, *A prism-based system for multippectral video acquisition*, viewed 11 January 2015, <https://homes.cs.washington.edu/~duhao/papers/multispectra_iccv2009.pdf>.

Fox, N 2001, 'Traceability to SI for EO measurements', *CEOS WGCV cal/val newsletter 9*, January 2001, pp. 1-9.

Gao, L, Kester, RT, Hagen, N & Tkaczyk, TS 2010, 'Snapshot image mapping spectrometer (ims) with high sampling density for hyperspectral microscopy', *Optical Express*, July 2010, pp. 14330-14344.

Hagen, N, Dereniak, EL & Sass, DT 2007, 'Fourier methods of improving reconstruction speed for ctis', *Imaging Spectrometry*, 2007, pp. 666103.1-666103.11.

Harvey, AR, Beale, JE, Greenaway, AH, Hanlon, TJ & Williams, JW 2000, 'Technology options for hyperspectral imaging', *SPIE Imaging Spectrometry VI*, 2000, pp. 13-24.

Hecht, E 2001, *Optics*, 4th edn, Addison Wesley.

Hege, K, O'Connell, DW, Johnson, SB & Dereniak, EL 2003, 'Hyperspectral imaging for astronomy and space surveillance', *Imaging Spectrometry IX*, 2003.

Johnson, WR, Wilson, DW, Fink, W, Humayu, M & Bearma, G 2007, 'Snapshot hyperspectral imaging in ophthalmology', *Journal of Biomedical Optics* 12, 2007.

Jupp, DLB 1997, *Issues in Reflectance Management*, CSIRO Earth Observation Centre, Discussion Draft August, viewed 15 April 2015, <http://www.eoc.csiro.au/millwshop/ref_cal.pdf>.

Kasap, SO 2001, *Optoelectronics and Photonics*, 1st edn, Prentice-Hall Inc, Upper Saddle River.

Kilpel, E 1981, 'Compensation of systematic errors of image and model coordinates', *Photogrammetria*, vol 37, pp. 15-44.

Krishnan, D & Fergus, R 2009, 'Dark flash photography', *SIGGRAPH*, pp. 96:1-96:11.

Leverington, DW 2001, 'Discriminating Lithology in Arctic Environments from Earth Orbit: An Evaluation of Satellite Imagery and Classification Algorithms', University of Manitoba, Manitoba.

Maloney, LT 1986, 'Evaluation of linear models of surface spectral reflectance with small numbers of parameters', *Optical Society of America*, vol 3, no. 10, pp. 1673-1683.

Milton, EJ 1987, 'Principles of field spectroscopy', *International Journal of Remote Sensing*, vol 8, pp. 1807-1827.

Milton, EJ, Rollin, EM & Emery, DR 1995, 'Advances in Field Spectroscopy', in FM Danson, SE Plummer (eds.), *Advances in Environmental Remote Sensing*, John Wiley and Sons, UK.

Mohan, A, Rasker, R & Tumblin, J 2008, 'Agile spectrum imaging: Programmable wavelength modulation for cameras and projectors', *Computer Graphics Forum*.

Moran, MS, Bryant, R, Thome, K, Ni, W, Nouvellon, Y, Gonzalez-Dugo, MP, Qi, J & Clarke, TR 2001, 'A refined empirical line approach for reflectance factor retrieval from Landsat-5M and Landsat-7 ETM+', *Remote Sensing of Environment*, October 2001, pp. 71-82.

Nicodemus, FE 1977, *Geometrical considerations and nomenclature for reflectance*, viewed 26 February 2015, <<http://physics.nist.gov/Divisions/Div844/facilities/specphoto/pdf/geoConsid.pdf>>.

Okamoto, T, Takahashi, A & Yamaguchi, I 1993, 'Simultaneous acquisition of spectral and spatial intensity distribution', *Applied Spectroscopy* 47, August 1993, pp. 1198-1202.

Park, J, Lee, M, Grossberg, MD & Nayar, SK 2007, 'Multispectral Imaging Using Multiplexed Illumination', *IEEE International Conference on Computer Vision (ICCV)*.

Richards, JA & Xiuping, J 1998, *Remote Sensing Digital Image Analysis*, 3rd edn, Springer, Canberra.

Salisbury, JW 1998, 'Spectral Measurements Field Guide', Defence Technology Information Centre, ADA362372.

Schaepman, ME 1998, 'Calibration of a Field Spectroradiometer. Calibration and Characterisation of a non-imaging field spectroradiometer supporting imaging spectrometer validation and hyperspectral sensor modelling', Department of Geography, University of Zurich.

Schaepman-Strub, G, Painter, T, Huber, S, Dangel, S, Schaepman, ME, Martonchik, J & Berendse, F 2006, 'About the Importance of the Definition of Reflectance Quantities - Results of Case Studies', *Remote Sensing Environment*, vol 103, no. 1, pp. 27-42.

Schechner, Y & Nayar, S 2002, 'Generalized Mosaicing: Wide Field of View Multippectral Imaging', *IEEE Transactions on Pattern Analysis and Machine Intelligence*, vol 24, no. 10, pp. 1334-1348.

Shepp, LA & Vardi, Y 1982, 'Maximum Likelihood Reconstruction for Emission Tomography', *Medical Imaging*, vol 1, no. 2, pp. 113-122.

Slater, PN, Biggar, SF, Holm, RG, Jackson, RD, Mao, Y, Moran, MS, Palmer, JM & Yuan, B 1987, 'Reflectance- and radiance- based methods for the in-flight absolute calibration of multispectral sensors', *Remote Sensing of Environment*, June 1987, pp. 11-37.

Snedecor, GW & Cochran, WG 1980, *Statistical Methods*, 7th edn, Iowa State Press, Ames.

Spiegel, MR 1992, *Theory and Problems of Probability and Statistics*, 2nd edn, McGraw-Hill, New York.

Appendix A: Project Specification

University of Southern Queensland

FACULTY OF ENGINEERING AND SURVEYING

ENG4111/4112 Research Project

PROJECT SPECIFICATION

FOR: **Scott Andrew MARSH**

TOPIC: REMOTE CONDUCTOR IDENTIFICATION

SUPERVISORS: Dr Leslie Bowtell
Dave Shephard, Regional Asset Manager, Ergon Energy.

ENROLMENT: ENG4111 – S1, D, 2015
ENG4112 – S2, D, 2015

PROJECT AIM: This project aims to investigate the use of hyper-spectral analysis to remotely identify overhead conductor material.

PROGRAMME: **(Issue B, 01 September 2015)**

- ❖ Research conductor metallurgy to identify the composite metals that make up commonly used overhead conductors.
- ❖ Critically evaluate current conductor identification techniques.
- ❖ Evaluate spectroscopy as a method of identifying overhead conductor materials under laboratory conditions.
- ❖ Attempt the construction of an image spectrometer using a consumer camera to further understanding and test the device on a conductor sample.
- ❖ Submit an academic dissertation on the research.

As time permits:

- ❖ Evaluate methods of remote conductor diameter measurement to use in conjunction with hyper spectral analysis to definitively identify overhead conductor.
- ❖ Investigate the feasibility of integrating conductor material identification and diameter measurement into the ROAMES LiDAR aircraft which overflies the entire Ergon Energy network each year.

AGREED _____(student) _____(supervisor)

Date: / /2015

Date: / /2015

Appendix B: Ocean Optics USB4000 Spec Sheet



Specifications

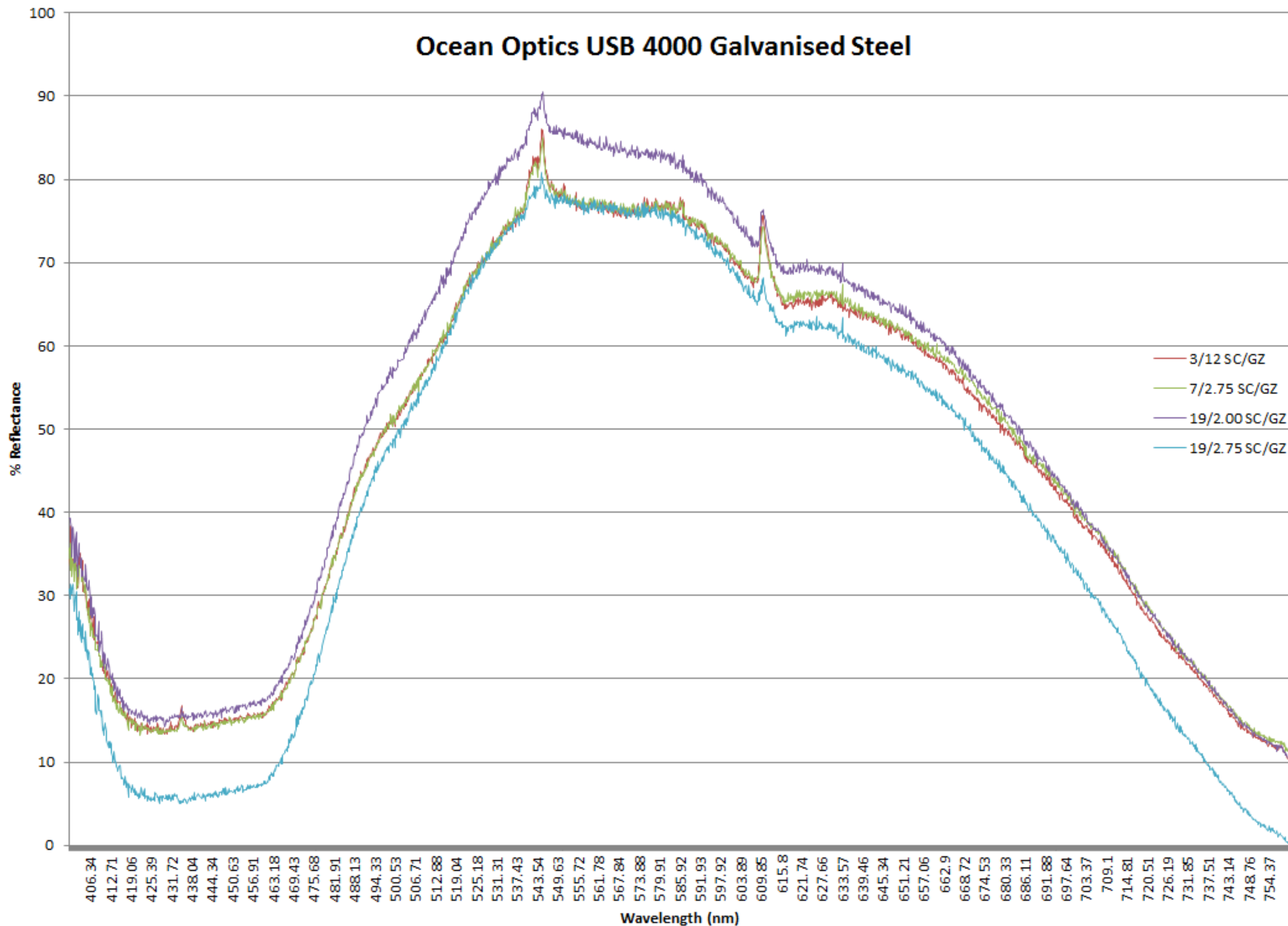
Specifications	Criteria
Absolute Maximum Ratings: V _{cc} Voltage on any pin	+ 5.5 VDC V _{cc}
Physical Specifications: Physical Dimensions Weight	89.1 mm x 63.3 mm x 34.4 mm 190 g
Power: Power requirement (master) Supply voltage Power-up time	230 mA at +5 VDC 4.5 – 5.5 V ~5s depending on code size
Spectrometer: Design Focal length (input) Focal length (output) Input Fiber Connector Gratings Entrance Slit Detector Filters	Asymmetric crossed Czerny-Turner 42mm 68mm (75, 83, and 90mm focal lengths are also available) SMA 905 14 different gratings 5, 10, 25, 50, 100, or 200 μm slits. (Slits are optional. In the absence of a slit, the fiber acts as the entrance slit.) Toshiba TCD1304AP linear CCD array 2 nd and 3 rd order rejection, long pass (optional)
Spectroscopic: Integration Time Dynamic Range Signal-to-Noise Dark Noise Resolution (FWHM) Stray Light Spectrometer Channels	10μs – 10 seconds 3.4 x 10 ⁶ (system); 1300:1 for a single acquisition 300:1 (at full signal) 50 counts RMS ~1.5 nm <0.05% at 600 nm; <0.10% at 435 nm One
Environmental Conditions: Temperature Humidity	-30° to +70° C Storage & -10° to +50° C Operation 0% - 90% noncondensing
Interfaces: USB RS-232	USB 2.0, 480 Mbps 2-wire RS-232

Appendix C: Nikon D700 Spec Sheet

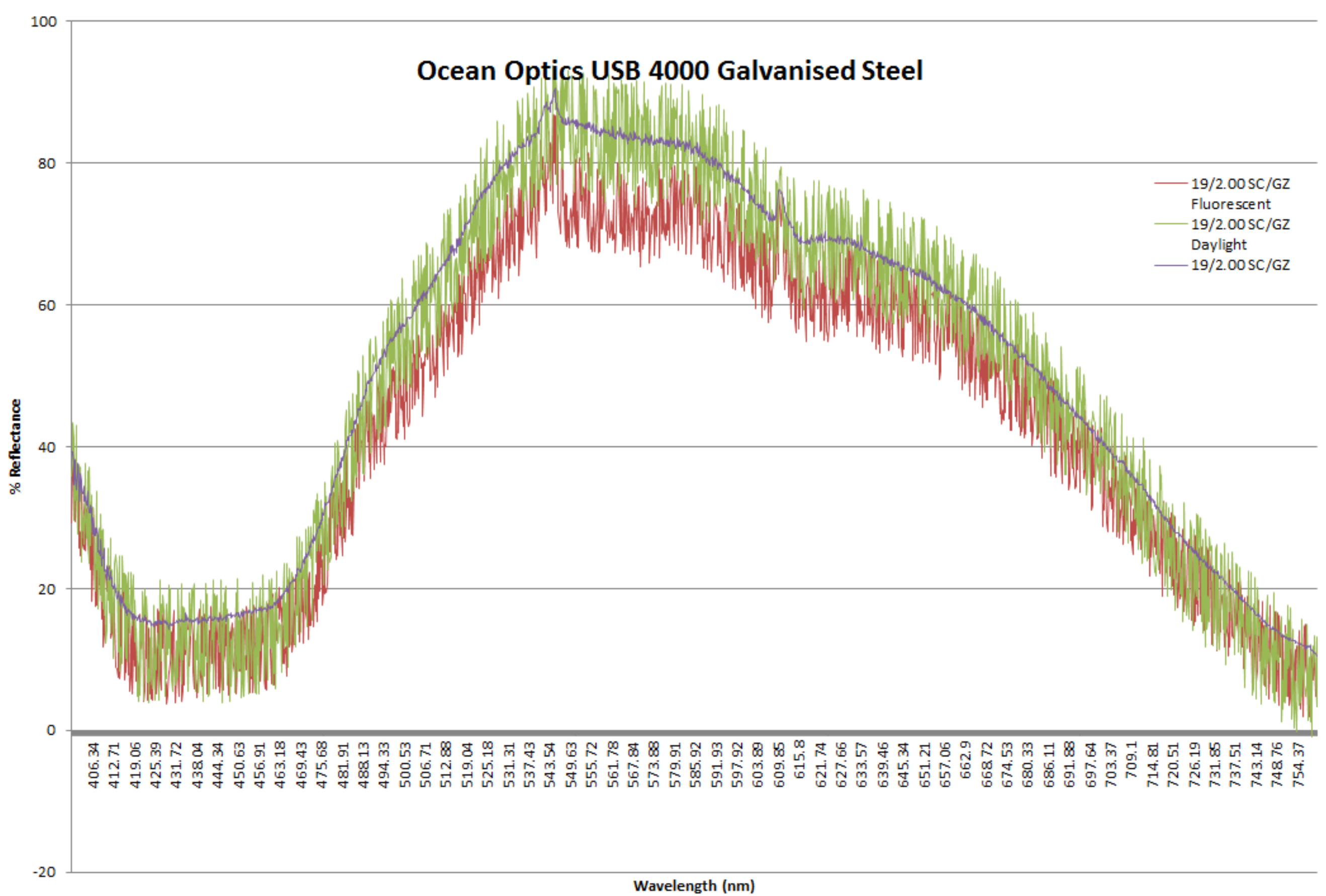
D700	
Key Features	Specifications
Effective pixels	12.1 million
Image sensor	CMOS sensor, 36.0 x 23.9 mm; total pixels: 12.87 million; Nikon FX format
Image size (pixels)	FX format (36 x 24): 4,256 x 2,832 [L], 3,184 x 2,120 [M], 2,128 x 1,416 [S] DX format (24 x 16): 2,784 x 1,848 [L], 2,080 x 1,384 [M], 1,392 x 920 [S]
Sensitivity	ISO 200 to 6400 in steps of 1/3, 1/2, or 1 EV; can be set to approx. 0.3, 0.5, 0.7, or 1 (ISO 100 equivalent) EV below ISO 200, or to approx. 0.3, 0.5, 0.7, 1 (ISO 12800 equivalent), or 2 (ISO 25600 equivalent) EV over ISO 6400
Storage media	CompactFlash (Type I, compliant with UDMA)
Monitor	3-in., approx. 920,000-dot (VGA), 170-degree wide-viewing-angle, 100% frame coverage, low-temperature polysilicon TFT LCD with brightness adjustment
Exposure metering	3D Color Matrix Metering II, Center-Weighted and Spot Metering
Exposure modes	Programmed Auto (P) with flexible program, Shutter-Priority Auto (S), Aperture-Priority Auto (A), Manual (M)
Interface	Hi-speed USB
Power sources	One Rechargeable Li-ion Battery EN-EL3e, Multi-Power Battery Pack MB-D10 (optional) with one Rechargeable Li-ion Battery EN-EL4a/4/3e, or eight R6/AA-size alkaline (LR6), Ni-MH (HR6), lithium (FR6) batteries, or nickel-manganese (ZR6) batteries
Dimensions (W x H x D)	Approx. 147 x 123 x 77 mm (5.8 x 4.8 x 3.0 in.)
Weight	Approx. 995 g (2.19 lb.) without battery, memory card, body cap or LCD monitor cover

* Specifications and equipment are subject to change without any notice or obligation on the part of the manufacturer. July 2008

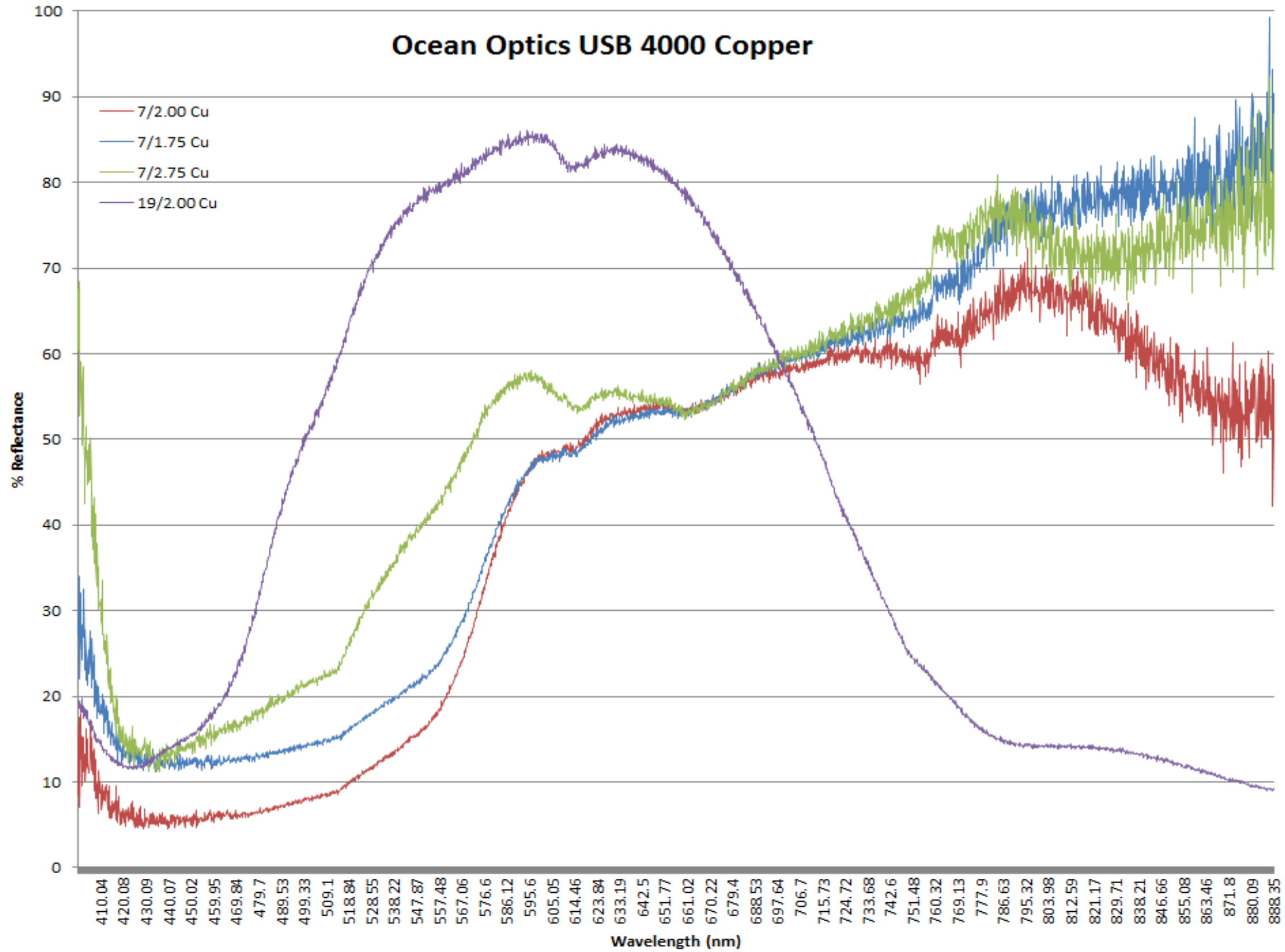
Appendix D: Ocean Optics USB4000 – Galvanised Steel Conductor under Halogen Spotlight



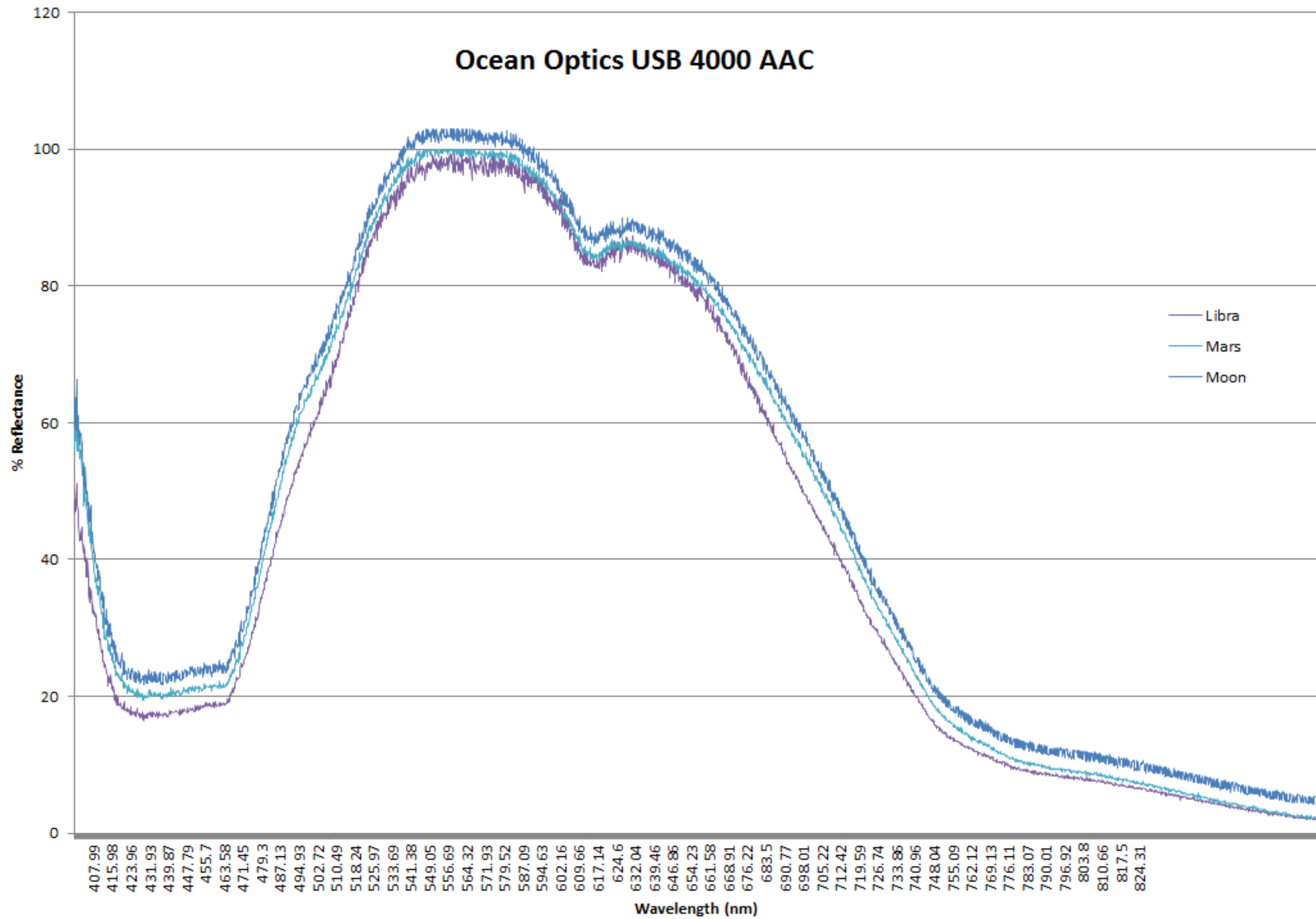
Appendix E: Ocean Optics USB4000 – Galvanised Steel Conductor under Halogen Spotlight, Fluorescent, and Low Level Daylight



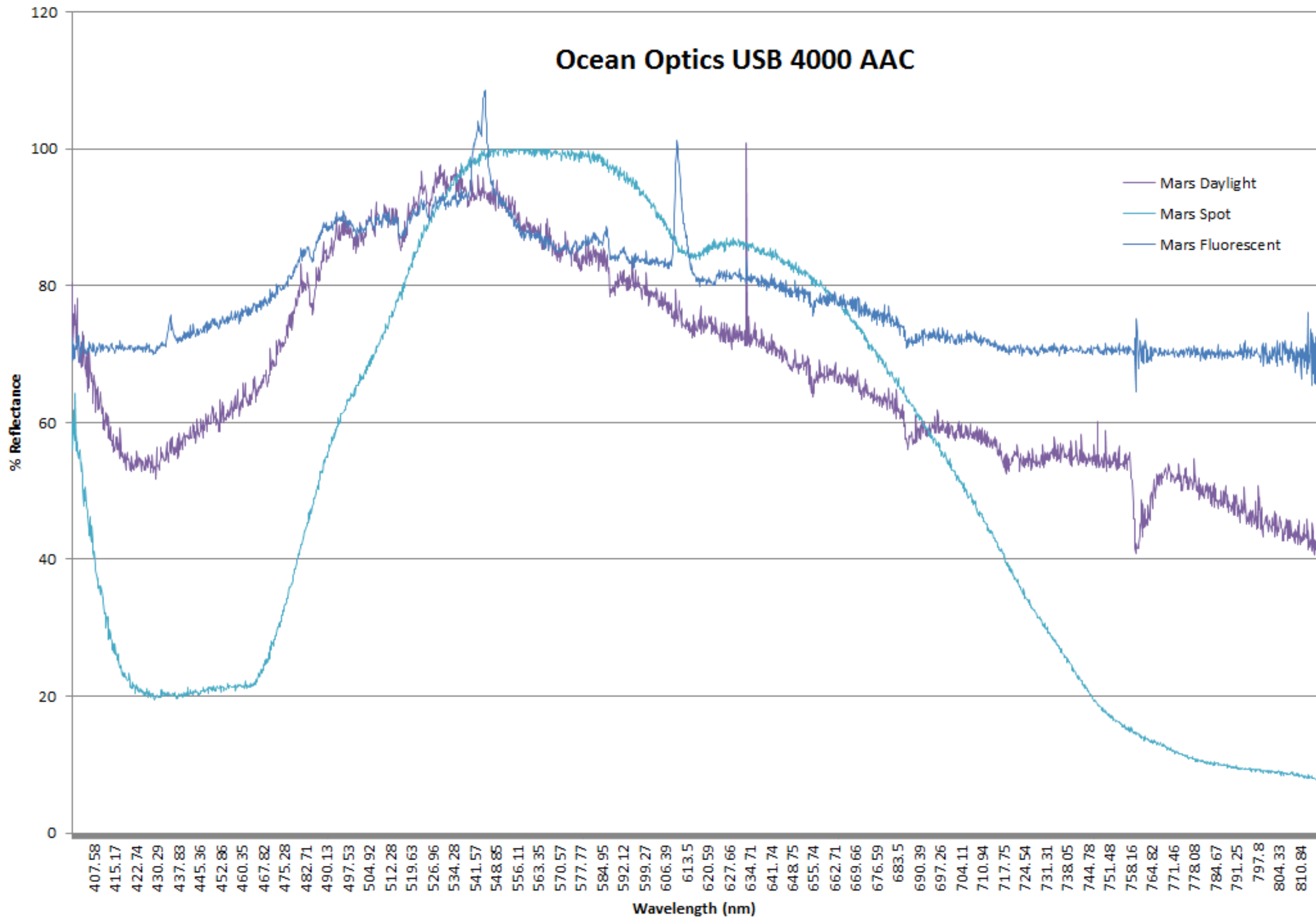
Appendix F: Spectroscopy Using an Ocean Optics USB4000 – Copper Conductor under Halogen Spotlight



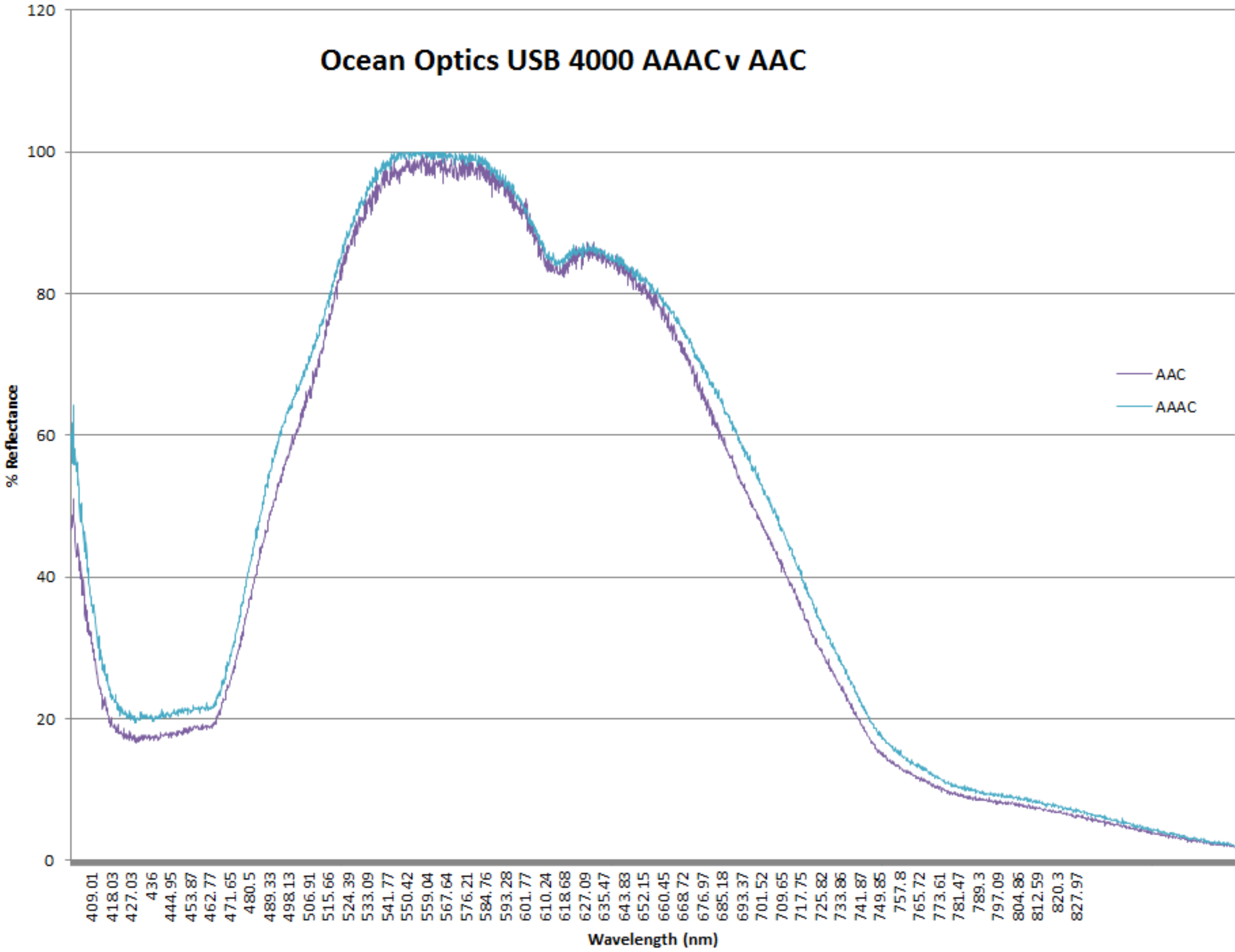
Appendix G: Spectroscopy Using an Ocean Optics USB4000 – Aluminium Conductor under Halogen Spotlight



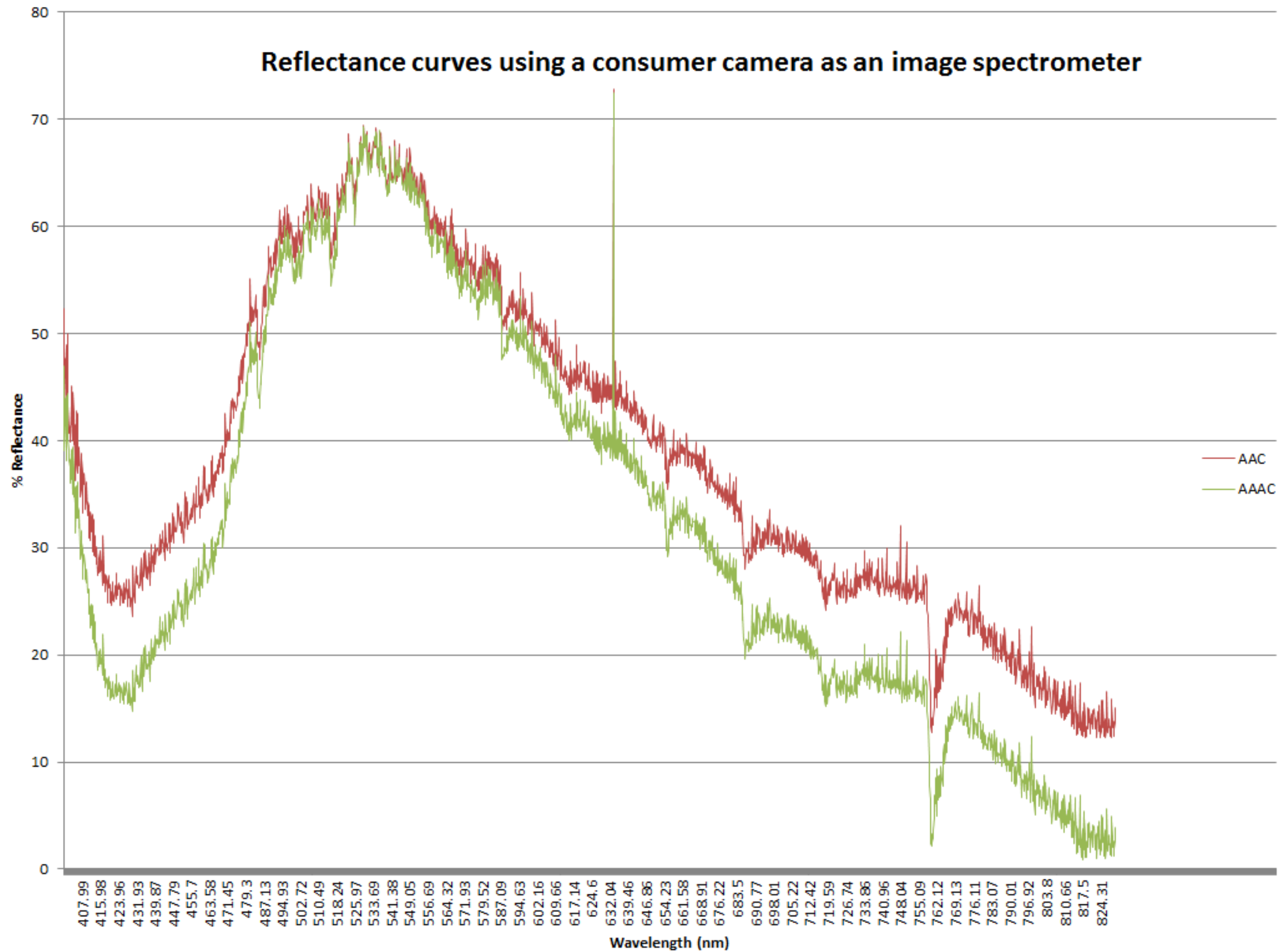
Appendix H: Ocean Optics USB4000 – All Aluminium Conductor under Halogen Spotlight, Fluorescent, and Low Level Daylight



Appendix I: Ocean Optics USB4000 – All Aluminium Conductor and All Aluminium Alloy Conductor under Halogen Spotlight



Appendix J: Image Spectroscopy Using a Consumer Camera – Confirmation of Concept



Appendix K: Spectroscopy Using an Ocean Optics USB4000 – All Conductors

